NUMERICAL MODELING OF AMASRA AND FATSA TSUNAMIS IN THE BLACK SEA

by

Esra Şahin

B.S., Geophysical Engineering, Kocaeli University, 2005

Submitted to the Kandilli Observatory and Earthquake Research Institute in partial fulfillment of the requirements for the degree of Master of Science

Graduate Program in Geophysics

Boğaziçi University

2013

ACKNOWLEDGEMENTS

First, I want to place on record, my sincere gratitude to Prof. Dr. Nurcan Meral Özel. As my thesis supervisor, she has shed light on my thesis research study and encouraged me at every point in the course of my study. I am very fortunate to have benefited from her perspectives and extensive experience.

I am also grateful to Prof. Ahmet Cevdet Yalçıner for his efforts to check my results and helpful advice.

With pleasure, I thank to Öcal Necmioğlu, Nilay Başarır and Ceren Özer for their precious helps, and their broad perspective. I would like to thank you to all the faculty members in the Geophysics Department for their support and help.

Personally, I would like to thank to my husband Sedat Şahin for his support and encouragement. Also, I would like to thank to my daughter Berra for her patience. Special thanks to my family, in particular, my mother and sister Nevin Tekcan and Nurcan Ağca. In addition, I thank to my dear friends Didem Barlas, Özge Can, Arzu Karasu, Nilüfer Kaya and Özlem Çelen as they have supported me every day.

ABSTRACT

NUMERICAL MODELING OF AMASRA AND FATSA TSUNAMIS IN THE BLACK SEA

Turkey, a country of frequent earthquakes and with a coastline of 8333 km, is also exposed to the tsunamis, resulting in material loss for the country and its neighbors (Altınok, 1999). Many new investigations have been performed for the tsunami research of the Black Sea region. According to historical data, there have been 26 tsunamis in the Black Sea since the first century; three of which occurred on the Turkish coast. Nine of these tsunamis occurred in the twentieth century (Altınok and Ersoy, 2000). Examining tsunami history and analyzing recent studies in the Black Sea will be crucial tasks for understanding tsunami generation and protecting coastal populations at risk.

Two historical tsunamis in the Black Sea have been investigated in this study, employing models obtained from the studies of each event: the Fatsa Tsunami, triggered by the Erzincan Earthquake (Ms=8.0, on 26 December 1939); and the Amasra Tsunami, triggered by the Bartın Earthquake (Ms=6.6, on 3 September 1968). Seismic source parameters of Erzincan and Bartın Earthquakes were investigated on the based of literature and data available for tsunami modeling purposes. In the study, tsunami models from two earthquakes occurred in sea and on land were generated by the NAMIDANCE Tsunami Simulation and Visualization code, using the seismic source parameters. In the Black Sea region, tsunami impact areas were presented by calculating tsunami arriving time, generation of wave, wave propagation and height of wave based on numerical simulation.

Furthermore this research compared previously existing tide gauge records from the North Black Sea, thought to be from the Fatsa Tsunami, with the results obtained from the tsunami models using numerical methods and sufficient agreement was found. For this reason, the available instrumental records of water surface fluctuations were digitized by

TESEO (Turn the Eldest Seismograms into the Electronic Original Ones) software (Pintore *et al.,* 2005). The tsunami waves generated from Erzincan Earthquake approaches the north coast between 40 min and 2.5 hours later. At the south coasts, maximum wave height is 0.34 m between Ordu and Fatsa towns.

In addition, the Amasra Tsunami was investigated in detail using tsunami model methodology and was evaluated its effects on the coasts of the Black Sea Region. Amasra Tsunami modeling studies indicates 0.80 m height of the initial wave.

Subsequently, the results of the tsunami models for both cases were compared and a general assessment of the tsunami hazard in Black Sea Region was provided.

ÖZET

KARADENİZ BÖLGESİ'NDE MEYDANA GELEN AMASRA VE FATSA TSUNAMİLERİNİN SAYISAL MODELLEMESİ

Bir deprem ülkesi olan Türkiye, 8333 km'lik sahil şeridi ile geçmişte ülkemizi ve komşularını etkileyen, maddi ve manevi kayıplara neden olan tsunami olaylarına maruz kalmıştır (Altınok, 1999). Karadeniz Bölgesinde meydana gelmiş tarihi tsunamileri konu alan araştırmalar yapılmıştır. Tarihsel verilere göre, Karadeniz Bölgesinde, dokuz tanesi 20. yüzyılda olmak üzere, birinci yüzyıldan günümüze 26 tarihsel tsunami kaydedildiğini göstermektedir (Altınok ve Ersoy, 2000). Karadeniz Bölgesinde meydana gelen tsunami olaylarının incelenmesi ve yapılan çalışmaların analiz edilmesi, bölgede tsunami oluşumunun anlaşılmasında ve kıyı yerleşiminin yoğun olduğu yerler için önlem alınmasında önemlidir.

Bu çalışmada, Karadeniz'in iki ayrı bölgesi için iki tarihi tsunami incelenmiş ve kaynak modelleme çalışmaları gerçekleştirilmiştir. 1939 Erzincan Depremi (Ms=8.0, 26 Aralık 1939) ile tetiklenen Fatsa Tsunamisi ve 1968 Bartın Depremi (Ms= 6.6, 3 Eylül 1968) ile tetiklenen Amasra Tsunamisi sismik verileri incelenerek, ulaşılabilen kayıtlar üzerinden kaynak parametreleri belirlenmiştir. Karada ve denizde gerçekleşen bu iki depremin saptanan kaynak parametreleri kullanılarak, tsunami modellemesi NAMIDANCE tsunami simülasyon programı ile gerçekleştirilmiştir. Tsunami dalgalarının oluşumu, dalganın yayılımı, belirlenmiş ölçü noktalarına dalganın varış zamanı ve yüksekliği modelleme çalışmaları sonucunda elde edilmiştir.

Araştırma kapsamında ayrıca 1939 Erzincan Depremi ile ilişkili Fatsa Tsunamisine ait olduğu düşünülen Kuzey Karadeniz mareograf (deniz seviyesi verileri) kayıtları TESEO (Turn the Eldest Seismograms into the Electronic Original Ones) (Pintore *et al.,* 2005) programı ile sayısallaştırılmıştır. Elde edilen deniz seviyesi zaman serileri tsunami

modellemesinin doğrulanmasında kullanılmıştır. Erzincan Depremi modelleme sonuçlarına göre tsunami dalgaları Karadeniz'in kuzey kıyılarına yaklaşık 40 dakika ve 2.5 saat arasında ulaşmaktadır. Güney kıyılarda maksimum dalga yüksekliği Ordu-Fatsa arasında 0.34 m olarak hesaplanmıştır.

Bartın Depreminin tsunami modellemesi ile ters faylanmalı deprem mekanizmalarının meydana getirebileceği tsunaminin güncel metodoloji ile ayrıntıları incelenerek, Karadeniz sahillerine olan etkileri değerlendirilmiştir. Amasra Tsunami modelleme sonuçlarına göre, ilk dalga yüksekliği 0.80 m hesaplanmıştır.

Erzincan ve Bartın Depremleri için tsunami modelleme sonuçları karşılaştırılmış ve genel bir değerlendirme yapılmıştır.

TABLE OF CONTENTS

LIST OF FIGURES

LIST OF TABLES

LIST OF ACRONYMS/ABBREVIATIONS

TESEO	Turn the Eldest Seismograms into the Electronic Original
wse	Water surface elevation
d	Depth
Lat	Latitude
Lon	Longitude
k	Tsunami intensity in Sieberg-Ambraseys 6-grade scale
K	Tsunami intensity in Papadopoulos-Imamura 12-grade scale
hmax	Max. wave amplitude

1. INTRODUCTION

Natural disaster mitigation needs to become a global priority. As the global population grows, so does the possibility of social and economic devastation resulting from natural disasters. Earthquakes, tsunamis, volcanoes, and submarine landslides are some of the growing dangers threatening human life. The effects caused by tsunamis have been widely observed globally, indicating that tsunamis can cause death and destruction both near their sources and at great distances away from them.

The majority of tsunamis have been generated in the Pacific Ocean. The Chilean tsunami of 1960 was one of the most destructive trans-Pacific tsunamis. The Great Tohoku Earthquake (Mw=9.0) on March 11, 2011, off the Pacific coast of Japan triggered powerful tsunami waves that reached maximum heights of up to 40.5 meters (Choi *et al.,* 2012). Although the majority of these tsunamis were generated in the Pacific Ocean, some destructive tsunamis have originated in the Indian and Atlantic Oceans too. In Indonesia, the 1883 Krakatau volcanic eruption generated the most widely known global tsunami. In 2004, the catastrophic and highly destructive Sumatran tsunami damaged the coastal regions of the Indian Ocean. The 1755 Lisbon Earthquake generated a tsunami with effects as far as the North Atlantic coasts (Baptista *et al.,* 2006).

Tsunamis have been observed in the inland seas such as the Mediterranean, the Aegean and the Black Sea. In the eastern Mediterranean, historical records can be traced back to the 15th century B.C.E. The volcanic eruption of Santorini produced a tremendous tsunami and, as a result, Minoan Civilization was entirely wiped out (Altınok and Ersoy, 2000). An M8.3 earthquake struck the southwestern part of the Hellenic Arc, near the Island of Crete, in AD 365, generating a tsunami that affected almost the entire eastern Mediterranean region (Eleftheria *et al.,* 2008). In 1303, the catastrophic earthquake that occurred in the Eastern Mediterranean area resulted in destruction on the Islands of Rhodes and Crete. In 1956, a strong earthquake in the Aegean Sea generated the most destructive Mediterranean tsunamis of the 20th century. Interest in tsunamis in marginal areas of the Mediterranean increased after the Izmit Bay tsunami triggered by the 19 August 1999

Kocaeli Earthquake. Historically, the most extensive tsunami information available has been from tsunamis reported along the Turkish coasts. The Istanbul Earthquakes of 1509 and 1894, the Eastern Marmara Earthquake in 1963, and the Izmit Earthquake in 1999 all wreaked havoc on the Marmara Sea. Furthermore, the 1939 Erzincan Earthquake in the Eastern Anatolia, and the 1968 Bartın Earthquake in the Western Black Sea, greatly affected sea levels in the cities of Fatsa and Amasra.

Research developments on tsunamis in the last decade have led to the recognition that tsunamis can pose a serious danger for Euro-Mediterranean coasts. The belt of the southern European countries all the way from Portugal to Greece and reaching east to Turkey, are mostly affected by tsunamis generated by local earthquakes. Local tsunamis attack the coasts immediately. This means that we must enact effective mitigation strategies for tsunamis in order to reduce reaction times. We must increase awareness of historical events in order to correctly infer what implications they may have for tsunami hazards.

The Black Sea region is a geographical area affluent in natural resources and strategically located in the center of Europe, Central Asia and the Middle East. The region has great development potential and is an important hub for energy and transport flows. Its regional significance is increasing and will continue to evolve. The region is the main fishery resource of Turkey while hosting country's major ports, industrial facilities, specific regional agricultural products (tea, tobacco and nuts), offshore oil and gas production barges and a number of planned nuclear power plants (Acır *et al.,* 2013).

This study also provides an important overview of the state of general understanding of tsunamis and tsunami studies for Turkish coasts of the Black Sea. Tsunami modeling was carried out for the Fatsa Tsunami triggered by the Erzincan Earthquake (Ms=8.0, on 26 December 1939) and Amasra Tsunami triggered by the Bartın Earthquake (Ms= 6.6, on 3 September 1968) in the Black Sea. The past tsunamis in the Black Sea have been well covered by certain publications. These publications describe many of the historical tsunami events (Altınok and Ersoy, 2000). They also detail source mechanisms of the Bartın Earthquake of 3 September 1968 and thoughts on active

tectonics of the Black Sea (Alptekin, *et al.,* 1986). Furthermore a preliminary estimate of tsunami risks was addressed in the Pelinovsky report of 1999, and indications of the spectra of the Black-Sea Tsunamis were analyzed in the S. F. Dotsenko and A. V. Ingerov report of 2007. Another report by S. F. Dotsenko and A. V. Ingerov report from 2007 looks at the characteristics of tsunami waves in the Black Sea according to the data of measurements. Another useful source has been tsunami in the Black Sea: Comparison of the Historical, Instrumental, and Numerical Data, detailed by A. Yalçıner *et al.* (2004).

Unlike those previously mentioned, this study compares existing tide gauge records from the northern coasts of Black Sea, thought to be from the Fatsa Tsunami, with the numerical results of Fatsa Tsunami modeling studies. Secondly, I focused on the tsunami caused by the Bartın Earthquake, which was triggered by the thrust fault mechanism investigated in detail by current numerical tsunami model methodology.

In the study, Tsunami models of two earthquakes generated information using the NAMIDANCE Tsunami Simulation and Visualization code. The tide gauge records from the north coast of the Black Sea were digitized by TESEO (Turn the Eldest Seismograms into the Electronic Original Ones) software (Pintore *et al.,* 2005).

This study will contribute to the tsunami studies in our country. Tsunami modeling will lead to a greater understanding of tsunamis and their characteristics in the studied regions. The identification of regions that will be affected by tsunamis will help them take the necessary precautions for handling the adverse impacts that might occur. This study will enable us to further understand Tsunami Disasters in Black Sea region.

From historical documents, it has been found that earthquakes produced tsunamis and caused material losses in Turkey and its vicinity. Tsunamis aren't frequent in Turkey, however to a certain degree they have a likelihood of occurring and it is still a possible threat for the coasts of Turkey. Without mitigation, future tsunamis have the possibility of causing greater damage than those historically occurring, and the increasingly dense coastal populations face a heightened risk.

2. TECTONIC FEATURES OF THE BLACK SEA AND PREVIOUS STUDIES

The Black Sea is a small intercontinental sea situated East-West between Europe and Asia. Its area is about $4.2x10^5$ km^2, the maximum water depth - 2.212 m. The length of the Black Sea shoreline is about 4.100 km (Figure 2.1).

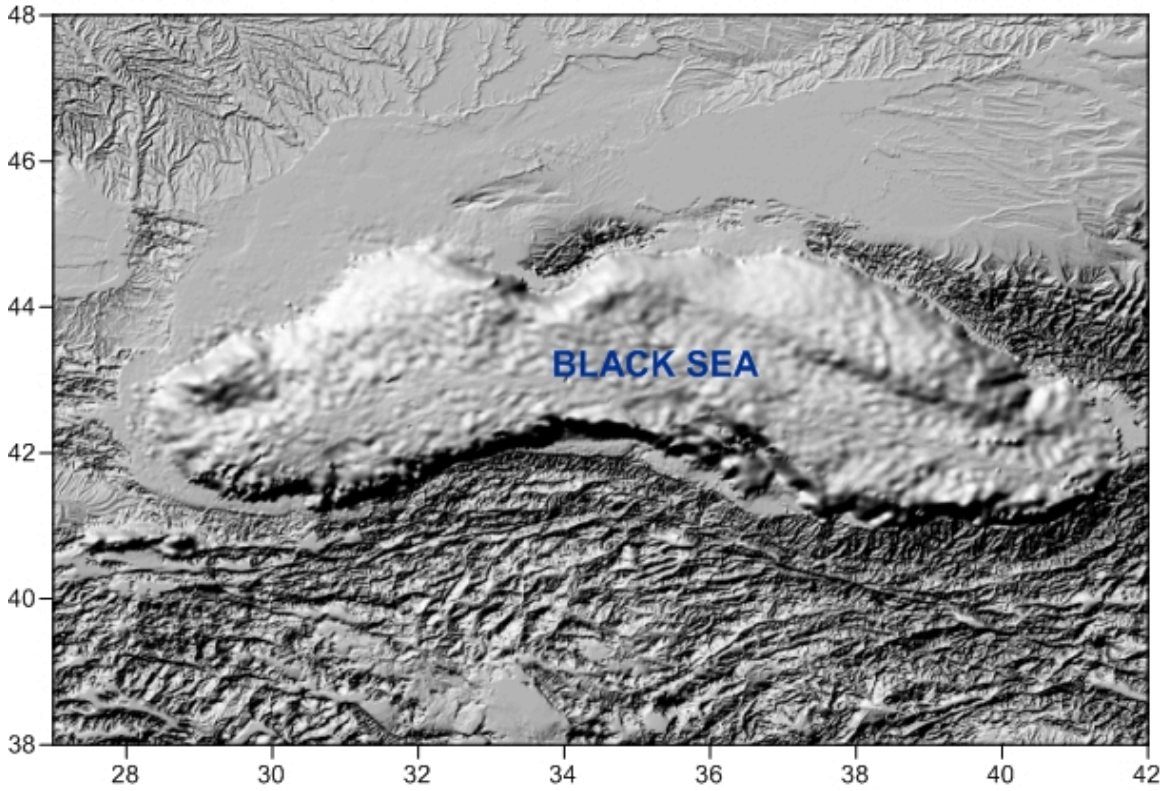

Figure 2.1. Location of the Black Sea.

Turkish portion of the Black Sea coastline has a length of 1650 km along and there are 15 cities. Six countries share a common coastline, Bulgaria, Romania, Ukraine, the Russian Federation, Georgia and Turkey (Figure 2.2).

Figure 2.2. Borders of the Black Sea neighboring countries (http://www.eoearth.org/article/Black_Sea).

The Black Sea basin is almost completely anoxic (without oxygen), containing oxygen in the upper 150 m depth and hydrogen sulphide in the deep waters. A permanent halocline separates the oxic (containing oxygen) and anoxic waters. The connection of the Black and Mediterranean Seas is limited to the Bosphorous- Dardanelles system of straits. In the Northeast, the Black Sea connects with the shallow Sea of Azov through the Kerch Strait. The Black Sea basin can be divided into four physiographic provinces: shelf (about 29.9 per cent of the total area of the sea), basin slope (27.3 per cent), basin apron (30.6 per cent), and abyssal plain (12.2 per cent). Figure 2.3 shows that summary of the geomorphologic zonation of the Black Sea.

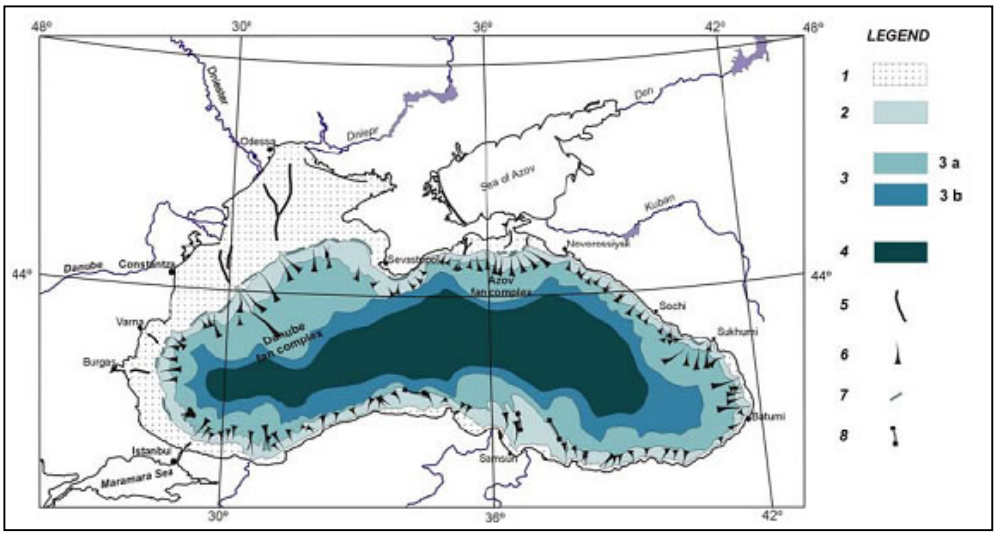

Figure 2.3. Geomorphologic zonation of the Black Sea (Panin and Ion, 1997). Legend; 1, continental shelf; 2, continental slope; 3, basin apron: 3 a - deep sea fan complexes; 3 b - lower apron; 4, deep sea (abyssal) plain; 5, paleo-channels on the continental shelf filled up with Holocene and recent fine grained sediments; 6, main submarine valleys - canyons; 7, paleo-cliffs near the shelf break; 8, fracture zones expressed in the bottom morphology.

One of the most prominent physiographic features is the very large shallow (less than 200 m deep) continental shelf within the north-western Black Sea (about 25 per cent of the total area of the sea). The Black Sea is located within a complex of high folded mountain chains of the Alpine system, which is represented by the Balkanides-Pontides belt to the south and by Caucasus, Crimea and the North Dobrogea Mountains to the north, north-east and the north-west respectively. Only in the Northwest, there are low-standing plateaus and the Danube delta lowland. Geologists consider the Black Sea a back-arc marginal extensional basin, which originated from the northward subduction of the Neo-Tethys along the southern margin of the Eurasian plate under a Cretaceous-Early Tertiary volcanic arc, as a result of the northward movement of the Arabic plate (Figure 2.4).

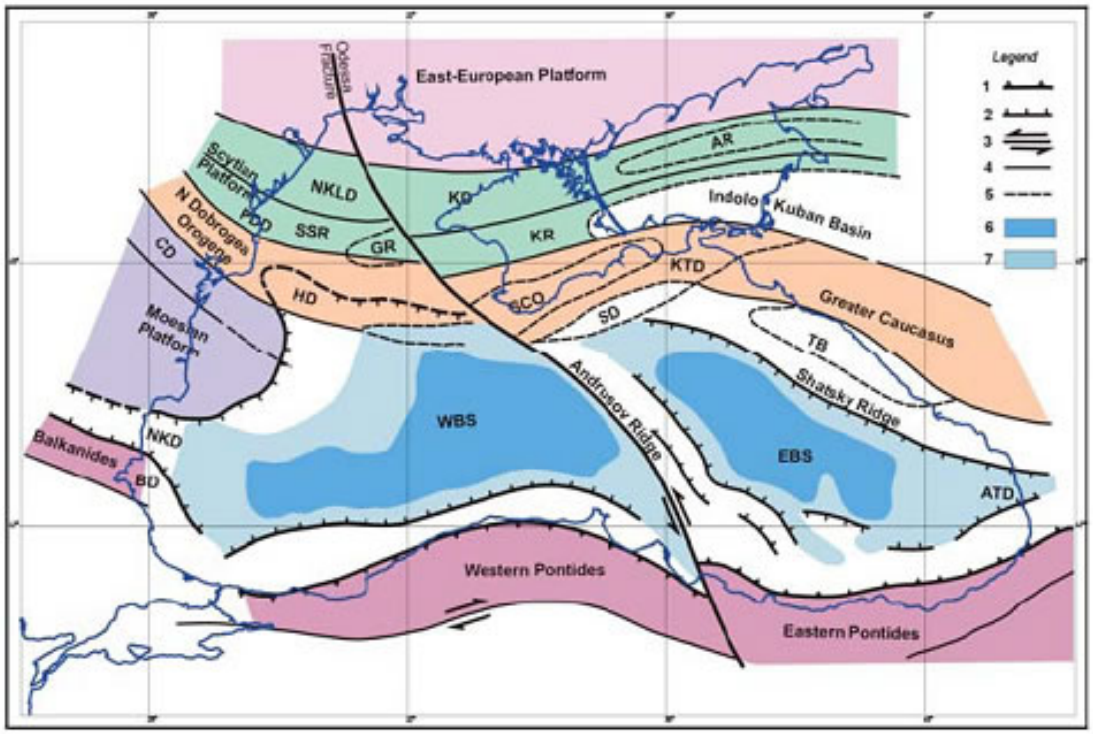

Figure 2.4. Tectonic sketch of the Black Sea Region (Panin *et al.,* 1994). Legend: 1, Orogene overthrust front; 2, Gravitational faults of the rift; 3, Major strike-slip faults; 4, Major faults; 5, Limits of depressions and/or ridges; 6, Zone without granitic crust; 7, Thinned crust.

Explanation of abbreviations: I. Platform regions: East European, Scytian, Moesian: II. Orogenic regions: North Dobrogea Orogene, Greater Caucasus, South Crimea Orogene – SCO, Balkanides, Western and Eastern Pontides; III. Depressions and ridges: PDD – Pre-Dobrogean Depression; NKLD – North Kilia Depression; KD – Karkinit Depression; HD – Histria Depression; SD – Sorokin Depression; KTD – Kerci-Taman Depression; NKD – Nijne-Kamchiisk Depression; BD – Burgas Depression; ATD – Adjaro-Trialet Depression; TB – Tuapse Basin; SSR – Suvorov-Snake Island Ridge; KR – Krymskyi Ridge; AR – Azov Ridge; GR – Bubkin Ridge; IV. WBS – Western Black Sea; V. EBS – Eastern Black Sea.

Since about 120 million years ago, the area has been a sea basin, with extremely dynamic development and huge sediment accumulation up to 13 km of bottom sediment

thickness in the central part of the basin. In the Black Sea, there are two extensional sub-basins with different geological history (Figure 2.4): the Western Black Sea Basin, which was opened by the rifting of the Moesian Platform some 110 Ma ago (Late Barremian) followed by major subsidence and probable oceanic crust formation about 90 Ma ago (Cenomanian) and the Eastern Black Sea Basin, with rifting beginning probably in the Late Paleocene (about 55 Ma ago), and extension and probable oceanic crust generation in the Middle Eocene (CA. 45 Ma ago) (Panin, 1996). There are two important seismic belts around the Black Sea. These are situated in northern Turkey (the North Anatolian Fault) and in the Caucasus region. The North Anatolian Fault is an east-west trending, highly active, right-lateral strike-slip fault. In the Caucasus region active folding and thrusting is observed (Kuşcu *et al.,* 2004).

2.1. Tsunami Hazard in the Black Sea

Tsunami prediction for the Black Sea is very challenging. Almost all historical tsunamis have been triggered within short distances from the coastline. The magnitudes of the tsunamigenic earthquakes in the Black Sea are not too high, and hence the tsunami impacts have been fairly local (Yalçıner *et al.,* 2004). They generally are induced by seaquakes with epicenters inside the sea, although, some were generated by the earthquakes with epicenters inland. Tsunamis in the Black Sea region have been mentioned in the several papers. Data on tsunamis occurring in the Black Sea and the Azov Sea from antiquity up to the present were updated, and compiled in the standard format developed since the 90's for the New European Tsunami Catalogue by Papadopoulos and Rangualev (2011). Twenty-six events were examined. Most of the events were generated in Crimea, offshore Bulgaria as well as offshore North Anatolia (Figure 2.1.1) Most of them were caused by earthquakes, such as the key event 544/545 of offshore Varna, but a few others were attributed either to seismic earth slumps or to unknown causes. The tsunami intensity was estimated using the new 12-grade scale introduced by Papadopoulos and Imamura (2001). From 544/545 up to now, only two reliable events of high intensity $K \geq 7$ have been reported, which very roughly indicates that the mean repeat time is ~ 750 years (K = tsunami intensity in Papadopoulos-Imamura 12-grade scale). Five reliable tsunamis of moderate intensity $4 \leq K < 7$ have been observed since 1650 up to the present, which

implies a recurrence of 72 years on the average. However, in the Black Sea there is no evidence of tsunamis of very high intensity (K ~ 10). This observation, along with the relatively low tsunami frequency, indicates that the tsunami hazard in the Black Sea is low to moderate but not negligible. The tsunami hazard in the Azov Sea is very low because of the very low seismicity but also because of the shallow water prevailing there. In fact, only three possible tsunami events have been reported in the Azov Sea (Papadopoulos *et al.,* 2011).

Figure 2.1.1. Sources of tsunami generation.

The first historical document about the Black Sea records a tsunami as early as the 1st century BC. When we look at the geographical distribution of Black Sea tsunamis, most tsunami reports center on the Crimea. The first such reports for Crimea refers to the 2nd century AD (103). During this tsunami occurred along the Sevastopol Bay, the sea first receded up to 0.5 km then returned. In the present century, the tsunami related to the earthquake of September 11, 1927 (M=6.8 ± 0.1) affected southern Crimea.

The tsunamis generated in the eastern part of the Black Sea are also important. One of the first documents on these is from 20 AD ± 20. It records that the tsunami associated

with an M 6.5 earthquake affected the gulf of Sukhumi; the sea rose up more than 2.5 m. The tsunamis during the earthquake of October 4, 1905 (M=5.1 ± 0.7) affected Anapa. In the same place, according to the records of 8 stations, another tsunami during the earthquake of July 12, 1966 (M=5.8 ± 0.5) resulted in some changes of sea level (Nikonov, 1997).

Up to now, there have been three tsunamis reported along the Black Sea coasts of Turkey. These were the Black Sea Tsunami of 1598, the Fatsa Tsunami of 1939 and the Amasra Tsunami of 1968 (Altınok and Ersoy, 2000). It is known that a tsunami in 1598 in the gulf between Sinop and Samsun connected with the Amasya-Çorum Earthquake, advanced the sea for 1.6 km inland on the coast of the Black Sea and drowned many people (Ambraseys and Finkel, 1995). On December 26/27, 1939, during the Erzincan Earthquake (M_s=8. 0), in Fatsa the sea receded 50 m and after a while the sea returned 20 m inland from the coast (Parejas *et al.,* 1942). The initial rise of sea level was recorded at 6 tidal stations on the northern coast of the Black Sea (Murty, 1977). Wedding (1968) stated that the sea inundated 100 m in Amasra and after the second wave advanced about 50-60 m from the shore during the Bartın Earthquake (M_s =6. 6) on September 3, 1968.

Tsunamis were also observed in the Sea of Azov, connected to the Black Sea. The first information is for the year 1650. The geological traces of the tsunami, which generated during an M=7 ± 0. 5 earthquake, were found in Sevastopol Bay. More recently there has been a 40 cm rise on the coast of the Sea of Azov on August 2, 1990 (Nikonov, 1997).

More than 20 tsunamis have so far been observed in the Black Sea. Nikonov (1997a, citing Grigorash and Korneva, 1972) stated that the wavelength in the Black Sea was 45-110 m, the velocity of travel was 120-140 km/h and the time of travel from one coast to the other was 10 to 110 minutes. When sufficient data can be compiled for the Black Sea, necessary precautions could be taken against tsunami hazards (Altınok and Ersoy, 1998).

2.2. Historical Data of Tsunamis in the Black Sea

The below section is the updated summary of tsunamis in the Black Sea that have occurred since the first century (Papadopoulos *et al.,* 2011).

2.2.1. 1st century, Sukhumi Bay/Colchis (West Georgia)

Coordinates: 43°00N, 41°00E

Nikonov (1994, 1997a, b) and Dotsenko (1995), based on Russian sources, reported that the submergence of the town of Dioskuriada on the coast of Sukhumi Bay, Colchis, in West Georgia today, can be inferred from both local legends and town remains in the bay bottom. A rapid subsidence by 2–3 m was related to a catastrophic earthquake of $M \geq 6.5$ occurring in the earlier half of the 1st century. It was suggested also that although no direct evidence for a tsunami was found, it may have occurred, judging from similar cases elsewhere on the globe, and that the run-up height exceeded 2.5m the tsunami intensity being k = IV−V. This information was also repeated by Pelinovsky (1999) and Yalçıner *et al.* (2004) who considered a tsunami intensity of k = IV−VI (k, tsunami intensity in Sieberg-Ambraseys 6-grade scale).

2.2.2. 1st century, Bizone (Kavarna, Bulgarian Black Sea coast)

Coordinates: 43°15 N, 28°12 E

Bizone was located where today named town of Kavarna is situated a few kilometers to the north of Balchik. Nikonov (1997b) reported that an early Armenian historian (Mowses Khorenatsi, 410–491 AD) mentioned a sudden flooding of the southern shores of the Black Sea back in the legendary times of the 1st century BC. Tsunami evidence is provided by sediment deposits found to the north of Varna at 43°18 N/28°18 E. The deposits were radiocarbon dated at about 2000 years and attributed to a large magnitude (M >7.0) earthquake (Ranguelov, 2003). Measurements indicated a wave run-up of 7–8 m.

2.2.3. 103 AD, Sevastopol Bay (Crimea)

Coordinates: 44°42N, 33°18E

Nikonov (1997a, b) based his conclusions on the St. Clements' miracles as well as on archaeological evidence for damage caused in settlements in the Sevastopol Bay, Crimea, and suggested that a strong earthquake of M~7 occurring at the beginning of the 2nd century AD, possibly in 103 AD, caused a strong tsunami in the bay. He estimated that the sea receded 500 m, and occasionally 3–4 km, and that the wave run-up was at least 2 m. The intensity of this tsunami was estimated of k = III (Nikonov, 1997a) or of K = III−IV (Yalçıner *et al.,* 2004).

2.2.4. 544/545, Odessus and Dionysopolis, Aphrodisium

Coordinates: 43°12 N, 28°18 E

A great flooding occurred in Varna Bay, Bulgaria, after an earthquake (speculative magnitude 7.5). According to Nikonov (1997), ''The sea had overflown its limits up to 4 miles onshore and had flooded the land in the region of Odessus (Varna), as well as the city of Dionysopolis (Balchik) and Aphrodisium (the city had been located on the Thracian Peninsula, near Saros Bay). Many people died in the seawater. Run-up heights exceeded 2–4 m. The intensity of this tsunami can be considered as intensity VIII–X according to the new tsunami intensity scale of Papadopoulos and Imamura (2001).

2.2.5. Autumn, 1185, Khan Konchak, Don River mouth, Azov Sea

Coordinates: 47°17 N, 39°13 E

This is an earthquake and tsunami event reported by Nikonov (1997) to have occurred at Khan Konchak near the mouth of Don River in the Azov Sea. That author concluded about the earthquake and tsunami occurrence from the interpretation of a passage from "*The Lay of Igor's Host*", a 12th century epic poem describing Prince Igor's campaign against the nomad tribes. Nikonov (1997) says: "*The passage from the poem speaks of the sea bursting out at midnight and clouds, chased by hurricanes . . .* " and "*the ground shook*

and moaned, rustling the tall grass, waking up the nomads in their camp . . . This occurred in the autumn of 1185 . . . ". However, the description is not convincing, particularly for the tsunami event, and is thus considered of low reliability by Papadopoulos (2011).

2.2.6. 1427, Yalta (South coast of Crimea)

Coordinates: 44°24 N, 34°18 E

From legendary and folklore accounts of the 15th century, Nikonov (1997) suggested that a very strong earthquake of M =7.0 ± 0.5 associated with a tsunami occurred around 1427 on the south coast of Crimea. It is said that several villages were washed away around the town of Yalta. Nikonov (1997) estimated the tsunami intensity at k = III and the water level rise on the shore of at least 2 m. Yalçıner *et al.* (2004) estimated intensity at K = II–IV. However, Papadopoulos (2011) reported that if the description "several villages were washed away" is correct, then the intensities k and K mentioned above underestimated the tsunami impact.

2.2.7. May 1598, Amasya (Central North Anatolia)

Coordinates: 40°24 N, 35°24 E

In 1598 a major earthquake occurred in central northern Anatolia (Ambraseys and Finkel, 1995). In some catalogues, this earthquake was referred to as Amasya and Corum earthquake (Altınok and Ersoy, 2000). The sea advanced for a mile inland on the coast of the Black Sea, drowning many people. The tsunami in the gulf between Sinop and Samsun reached up to 1 m wave height (Altınok and Ersoy, 2000). The intensity of this tsunami can be considered as intensity II–IV according to the new tsunami intensity scale of Papadopoulos and Imamura (2001).

2.2.8. 5 June 1615, Feodosia (SW Crimea)

Coordinates: 44°54 N, 35°30 E

Based on Armenian chronicles, Nikonov (1997a) listed an earthquake of M = 6.0±0.5 and an associated tsunami occurring on 5 June 1615 on the southeastern coast of Crimea with the next description: "*Swell, sea level rise and recession to the ordinary level near the town of Feodosia.*" He also estimated the water level rise to be 0.5 to 1.0 m and the tsunami intensity k = II. According to Yalçıner *et al.* (2004), the tsunami intensity K was estimated between II and IV.

2.2.9. 1650, Sivash (Azov Sea)

Coordinates: 44°42 N, 33°18 E

This was an earthquake (M =7.0 ± 0.5) and tsunami event reported by Nikonov (1997) to have occurred in 1650 in the western shores of the Azov Sea as well as in the Black Sea: "*Sea flooded the shore to connect with the Sivash, then the water receded near Genichesk and Arabat. Geological traces of tsunami in the Sevastopol Bay*" in Crimea. He also estimated a water level rise of 0.5 to 1.0 m and a tsunami intensity k of degree III.

2.2.10. 12 October 1802, Evpatoria (western Crimea)

Coordinates: 45°42 N, 26°36 E

Large waves near the beach at Evpatoria, Crimea, Ukraine, were observed on 26 October 1802, when sea was calm. It was reported that these waves were triggered via an earthquake with speculated magnitude 7.5 (Nikonov, 1997).

2.2.11. 17 November 1821, Odessa (Ukraine)

Coordinates: 47°00 N, 29°12 E

On 17 November 1821 an earthquake took place in the south of the Russia. It continued for 40 s in Odessa, Ukraine. ‘‘The sea exceeded its standard level’’ (Nikonov, 1997).

2.2.12. 23 January 1838, Odessa (Ukraine)

Coordinates: 45°42N, 26°36E

This was another large, intermediate-depth earthquake of an estimated magnitude of 7.3 occurring at the Vrancea seismic source, Romania (Constantinescu and Marza, 1989). The earthquake became perceptible at long distances but not so far away as the 1802 one (Von Hoff, 1841; Mallet, 1855). In Transylvania the buildings first rocked from side to side and then the walls cracked and fell. From Russian sources, Nikonov (1997) listed the earthquake and an associated sea disturbance: "*Strong sea swell damaging many vessels in the Odessa harbor.*" He estimated a tsunami intensity of k = II. Yalçıner *et al.* (2004) based their findings on the information provided by Nikonov (1997) and estimated a tsunami intensity of K = VII–VIII degree on the new 12- grade scale of Papadopoulos and Imamura (2001).

2.2.13. 11 November 1869, Sudak and Evpatoria (Crimea)

Coordinates: 44°42N, 35°00E

Based on Russian sources, Nikonov (1997) listed a shallow earthquake (M = 6.0 ± 0.2) and a tsunami event in Crimea: "*Town of Sudak: a violent horizontal recession of the sea by 2m and a slow return to the ordinary level in 10 min. A strong tidal wave as high as 1m near the town of Evpatoria.*" He estimated tsunami intensity to be k = I–III. Again from Russian sources, Dotsenko (1995) described the event shortly as follows: "*The earthquake had intensity 7–8 in Yalta, Sevastopol and Sudak. The sea was stormy*" (Pelinovsky, 1999). Yalçıner *et al.* (2004) summarized the above information and estimated that the intensity of this tsunami can be considered at K = II–IV. Earthquake parameters were adopted from Nikonov (1997).

2.2.14. 25 July 1875, Western coast of Crimea

Coordinates: 44°30N, 33°18E

A Russian source indicated that a moderate earthquake of M = 5.5 ± 0.5 caused some sea

disturbance with estimated tsunami intensity k = I–III: "*Western coast of Crimea. Water was agitated and foamed*" (Nikonov, 1997). Yalçıner *et al.* (2004) summarized the information provided by Nikonov (1997) and estimated that the intensity of this tsunami could be considered at K = II–III. The earthquake parameters were adopted from Nikonov (1997).

2.2.15. 31 March 1901, Balchik (North Bulgarian Black Sea Coast)

Coordinates: 43°24N, 28°42 E

A large earthquake of M =7. 1 and maximum intensity of X degree occurred offshore Shabla- Kaliakra, NE Bulgaria, causing surface landslides of several km and subsidence of about 3 m. "*The boats in the port of Balchik were uplifted about the same altitude*" (Ranguelov, 1996). This information came from an eyewitness reviewed in early 70's by B. Ranguelov, (1996). Tsunami inundation with a maximum height of about 2.5–3 m was reported by an eyewitness at the Balchik port (Grigorova and Grigorov, 1964).

2.2.16. 4 October 1905, Anapa (NE Black Sea)

Coordinates: 44°42 N, 37°24 E

From Russian sources, sea waves were described in association with a moderate (M = 5.1) earthquake near Anapa: "*NE coast of Black Sea near the town of Anapa. Waves off Anapa shook up a ship. Maximum water level rise* ≥ 0.5 *m, k=II. Earthquake magnitude* M = 5.1 ± 0.7" (Nikonov, 1997); "*Submarine earthquake of* M = 7 *was registered in the vicinity of the town of Anapa, Russia. The waves were so large at the sea surface that they bounced the vessel. Five shocks were felt*" (Grigorash and Korneva, 1969; also Dotsenko, 1995; Pelinovsky, 1999). The intensity of this tsunami can be considered at K = III–VI (Yalçıner *et al.,* 2004).

2.2.17. 8 April 1909, Cape Idokopas (Western Caucasus)

Coordinates: 44°15 N, 38°07 E

Nikonov (1997) based his findings on a Russian source and described an aseismic case of sea waves observed off the coast of Western Caucasus: "*Off the NE coast of Black Sea near Cape Idokopas. Three waves off Cape Idokopas.*" Although no information was provided about the features of the wave, he suggested that tsunamis may arise in the Black Sea not only from large seismic events, but also from underwater slides, and that this was most likely the cause of the 1909 tsunami when the wave height in the open sea above the continental slope reached 3–5 m. To support his suggestion, Nikonov (1997) noticed that an underwater cable broke twice due to moderately sized earthquakes that occurred in the NE Caucasus in 1870. He added also that abundant turbidities in near-surface sea deposits off the Caucasian, Crimean, and Bulgarian coasts also confirmed the conclusion that underwater slides occurred there. In fact, a recent case observed along the Bulgarian coast in 2007 was described and studied by Ranguelov *et al.* (2008).

2.2.18. 26 June 1927, Yalta (South Crimea)

Coordinates: 44°24 N, 34°24 E

Data published in Russian sources have shown that a strong earthquake with a magnitude of 6.0 occurred possibly on the submarine slope south of Yalta and caused a local tsunami on the south coast of Crimea. Dotsenko (1995) and Konovanov (1996) published data from Soviet tide-gauge stations that recorded the event with maximum height of 24 cm at Yalta station, the heights in another five stations ranging from 6 to 14 cm. Eye witnesses noted that the sea bottom topography changed with the earthquake by a downward shift of silt on submarine rocks along the Crimean coastal zone, and that "*changes in the sea level in the western and eastern parts of the Kerch Strait and, in general, the sea was stormy and rough throughout the entire earthquake*" (Dotsenko, 1995, from various Russian sources; also Pelinovsky, 1999). According to the data collected by Nikonov (1997), in the Gurzuf village the sea receded by 1.5 m, then came back again to the shore. In Yalta, the sea level fell by 0.18 m and then rose by 0.16 m. In Sevastopol, a maximum sea level rise of 0.16–0.32 m was observed. In Alupka, the sea receded and then returned onto the shore and

overwhelmed the beach. Sea disturbance was also reported from Feodosia, Alushta, Tuapse, Sudak, Novorossiysk and Kerch. The intensity of this tsunami was estimated at k = II (Nikonov, 1997) or K = III–IV (Yalçıner *et al.,* 2004). Considering the eyewitness, Papadopoulos supported that the tsunami of 26 June 1927 was triggered by submarine slumps initiated by the earthquake.

2.2.19. 11 September 1927, South Crimea

Coordinates: 44°18 N, 34°18 E

After the event on 26 June 1927, an even larger and destructive earthquake of magnitude 6.5 occurred in the Crimean region. The epicenter co-ordinates were situated on the slope of the Black Sea trough, 20 km southeast of Yalta. In the open sea, near the seismic source, fishermen observed sea surface variations and roughness (Dotsenko, 1995; Pelinovsky, 1999). From several Russian sources reviewed by Nikonov (1997) it results that in Balaklava, to the south of Sevastopol, the sea receded in the bay by 0.6–1.0 m, then rushed onto the shore and overwhelmed a vast expanse (15 m) rising by 0.5 m; two houses were destroyed. In Sevastopol, ebb up to 0.5 m was observed, while in Yalta first a rapid fall and then oscillation at 0.37 m were reported. Sea level rise was also reported in other localities. The earthquake was accompanied by tsunami waves recorded on tide gauges with a height of 39 cm in Evpatoria, 35 cm in Yalta, 23 cm in Sevastopol, 18 cm in Novorossiisk and Tuapse, and 20 cm in Batumi (Dotsenko and Konovanov, 1996). The intensity of this tsunami was estimated as k = II by Nikonov (1997).

2.2.20. 16 September 1927, South Crimea

Coordinates: 44°18N, 34°00E

An aftershock, magnitude of 4.9 of the main shock, 12 September 1927, caused the sea water to recede and then to rise more than 0.3 m in the bay of Balaklava. The intensity of this tsunami was estimated at k = II (Nikonov, 1997) or K = III–IV (Yalçıner *et al.,* 2004) in the new 12-grade scale introduced by Papadopoulos and Imamura (2001).

2.2.21. 26 December 1939, Fatsa (Black Sea coast of North Turkey)

Coordinates: 39°30N, 39°30 E

This earthquake (M = 7.9) occurred at 23:57GMT of 26 December 1939 rupturing a long segment of the North Anatolian Fault. Loss of life was reported 40 000 (Altınok and Ersoy, 2000); over 30 000 dwellings were destroyed. The four largest communities where the majority of structures were destroyed were (from east to west) Ercincan, Suşehri (Endires), Misas, Reşadiye, and Niksar (Neocaesarea). Parejas *et al.* (1942) and Altınok *et al.* (2000) mentioned that a person in Fatsa, to the east of Sinop, wanted to dive into the sea instinctively at the time of the earthquake, but he was not able to reach the sea because it had receded about 50 m. According to observations collected by Altınok and Ersoy (2000) during the earthquake the sea receded 100m in Ünye and sunken rocks appeared for the first time. The sea also receded for 50–60 s in Giresun. Moreover, in Ordu, the people at the harbour saw that the sea initially became quiet, than receded about 15 m. The level of the sea returned to normal in 5–10 min. The tsunami crossed mainly the eastern part of the Black Sea and was recorded on tide gauges in Soviet harbors. Yalçıner *et al.* (2004) estimated that the intensity of this tsunami can be considered K = III–V while Nikonov (1997) tentatively estimated k = IV. That the rupture zone of the earthquake is situated a long distance inland from the north coast of Turkey, where the tsunami was observed, makes it difficult to understand the tsunami generation mechanism. This is exactly why Richter (1956) noted that since the main shock epicenter was certainly on land, the sea motion in Fatsa is important. Pelinovsky (1999) proposed three possibilities as for the tsunami source: (i) ground rupture, (ii) secondary fault believed to be associated with the dislocation motion in the Black Sea, (iii) submarine landslide triggered by the earthquake in the Black Sea. Yalçıner and Pelinovsky (2004) investigated the possible source mechanism by comparing results of the numerical modeling of the tsunami with the observational data and the instrumental records, but they did not reach a conclusive result.

2.2.22. 12 July 1966, Anapa (Crimea)

Coordinates: 44°42 N, 37°12 E

This was a tsunami triggered by a moderate earthquake (M = 5.8) occurred about 10 km

offshore Anapa at a focal depth of 55 km. Tsunami wave was recorded by Soviet tide gauges. The highest amplitudes were 42 cm in Gelendzhik, at 50 km to the south, and 10 cm in Feodosia at 60 km across the Crimean Peninsula. The intensity of this tsunami can be considered k =I (Nikonov, 1997) or K = III–V (Yalçıner *et al.,* 2004) and submarine slump is a more likely mechanism. At this point, it is of relevance to note that Dotsenko and Ingerov (2007) studied the digitized records and the spectral features of the 26 July 1927, 11 September 1927, 26 December 1939 and 12 July 1966 tsunami waves. They found that as a rule, tsunami waves were characterized by the initial elevation of the sea level and that the height of the first wave was not the maximum one. The maximum heights of the recorded tsunami waves at the points of observation did not exceeded 52 cm. For the major part of points on the coast, they observed a noticeable trend towards increase in the heights of waves with the magnitude of the earthquake.

2.2.23. 3 September 1968, Amasra (Black Sea coast of north Turkey)

Coordinates: 41°49 N, 32°23 E

The Bartın Earthquake was strong (M = 6.6) and destructive, killing 24 persons. During this earthquake on the Black Sea north coast of Turkey, the precipitous coastline between Amasra and Çakraz uplifted by 35–40 cm, and the sea level lowered on the coastal rock. Lander (1969) reported that the sea receded 12 to 15 m in Çakraz at the onset of the earthquake and never returned entirely to its original level. Wedding (1968; after Altınok and Ersoy, 2000) stated that the sea inundated 100 m in Amasra and after 14 min the second wave inundated the shore about 50–60 m. This wave dragged many objects and caused many boats to be stranded. The silent and unstopped progression of the sea frightened the population. The reason for this progression was most probably the uplifting around Çakraz. According to Yalçıner *et al.* (2004), the intensity of this tsunami can be considered as K = III–V on the new tsunami intensity scale of Papadopoulos and Imamura (2001). The coastal uplift between Amasra and Cakraz is consistent with the fact that the modelling of P and SH seismic waves showed earthquake focal mechanism of thrust type and very shallow source, the focal depth being 4 km (Alptekin *et al.,* 1986, Altınok and Ersoy, 2000).

2.2.24. 4 December 1970, Sochi (eastern Black Sea)

Coordinates: 43°42N, 38°30Coordinates: 43°42N, 38°30E

A moderate earthquake (M =5.1) occurred at 01:59GMT caused a rapid sea level rise at 05:20 local time (LT), a maximum rise by 34 cm at 06:05 LT and a maximum fall of 45 cm at 06:10 LT near the town of Sochi (Dobrychenko *et al.,* 1975; after Nikonov, 1997). However, it is not clear if these observations were macroscopic or from tide-gauge records, which is likely the case. Tsunami intensity of k = I–II was estimated by Nikonov (1997). Yalçıner *et al.* (2004), apparently based on the previous Russian sources reported "*sea oscillations with heights of 80 cm and period of 5 min.*" The data available are not sufficient to suggest a possible generation mechanism for the sea level changes.

2.2.25. 2 August 1990, southern coast of the Azov Sea

Coordinates: 45°38N, 36°31E

A sudden, short-lived sea level rise of 40 cm was observed on the southern coast of the Sea of Azov (Nikonov, 1997a). A tsunami intensity of k = II was estimated by Nikonov (1997).

2.2.26. 7 May 2007, Bulgarian Black Sea coast

Coordinates: 43°06N, 28°36E

According to Ranguelov *et al.* (2008), a tsunami-like sea disturbance of non-seismic origin was observed on 7 May 2007 on the Bulgarian Black Sea coast from north to south, a distance of about 150 km, but it was stronger to the north. Turbulence, strong water currents, mud waters and foam in some sites (*e.g.,* in Balchik and Kavarna) were described. The chief period of the oscillations was between 4 and 8 min. at most places. The maximum sea level rising and lowering were +1.2 m and −2.0 m, respectively. Many small fishing boats were cast onto the beach in Kavarna and Balchik Marinas. Several accounts of eyewitnesses as well as reports of local port authorities and three tide-gauge records were available, collected and analyzed by the above authors who thought that the tsunami was produced either by a submarine landslide or by atmospheric pressure pulses.

3. GENERAL INFORMATION ON TSUNAMI AND NUMERICAL MODELING STUDY IN THE BLACK SEA

3.1. General Information on Tsunami

The tsunamis are long waves generated by any large, abrupt disturbance of the sea surface. Tsunami waves are generated as a result of various causes, such as an earthquake rupture process or, the secondary triggered phenomena, such as landslides (submarine or surface) and occur rarely that volcanic eruptions and asteroid impacts (Bernard, 2007). The tsunami computations are principally based on the long wave theory (Shuto, 1990). When tsunamis are generated and begin to propagate in deep sea, they initially show a behavior that is described by linear long wave theory. While approaching to the shoreline, the tsunami wave height increases with the reduction of its velocity and wavelength decreases, then the nonlinear effects become significant. When tsunamis reach to the land, the effects of hydrodynamic parameters become significant (Özer, 2012). Figure 3.1.1 demonstrates the sectional view of tsunami inundation zone with the hydrodynamic parameters as water surface elevation, flow depth, run up and inundation distance. As seen from the figure, water surface elevation is specified with respect to still water level while the flow depth is stated relative to the ground level.

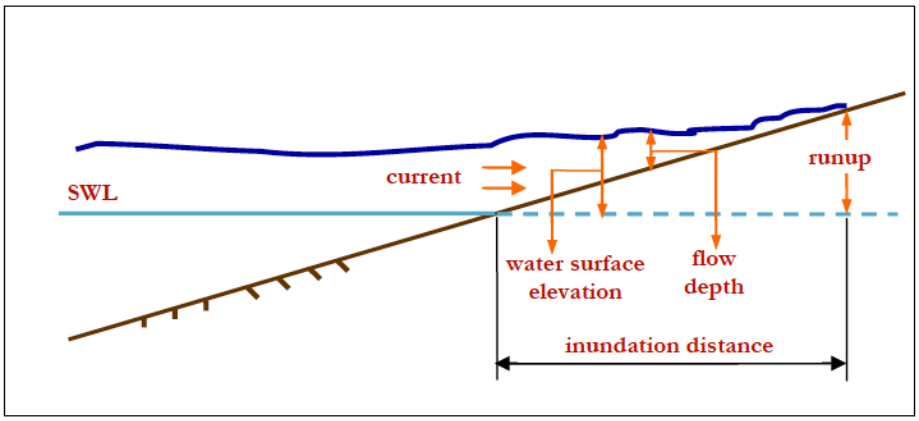

Figure 3.1.1 Sectional view of tsunami hydrodynamic parameters, (Özer, 2012).

3.2. Numerical Modeling Study in the Black Sea

In the Black Sea, tsunami models of two earthquakes, the Bartın Earthquake (Ms= 6.6, on 3 September 1968) and the Erzincan Earthquake (Ms=8.0, on 26 December 1939), occurred in sea and on land, respectively, were generated by the NAMIDANCE code. NAMIDANCE is a computational tool developed by Andrey Zaytsev, Ahmet Yalçıner, Anton Chernov, Efim Pelinovsky and Andrey Kurkin for tsunami modeling. It provides direct simulation and efficient visualization of tsunamis to the user and for assessment, understanding and investigation of tsunami generation and propagation mechanisms. The model creates the initial wave (wave form at a result of earthquake rupture at the sea bottom and finite principle equation, based on Okada (1985) calculations) by using not only tsunami genic rupture parameters of earthquake but also user defined dimensions and shapes of the initial water surface disturbance. It is based on the solution of nonlinear form of the long wave equations subject to initial and boundary conditions (http://namidance.ce.metu.edu.tr). It computes all necessary parameters of tsunami behavior in shallow water and in the inundation zone allowing for a better understanding of the effect of tsunamis according to bathymetric and topographical conditions (Yalçıner *et al.,* 2006). The major tsunami hydrodynamic parameters, such as maximum water surface elevations (positive and negative tsunami amplitudes) were calculated by inserting the numerical model NAMI DANCE.

3.3. Capabilities of NAMIDANCE

NAMIDANCE computes tsunami source from either rupture characteristics or pre-determined wave form, tsunami propagation, arrival time of tsunami wave, coastal amplification, time histories of water surface fluctuations at selected gauge locations, inundation (according to the accuracy of grid size), distribution of current velocities and their directions at selected time intervals, distribution of water surface elevations (sea state) at selected time intervals, relative damage levels according to drag force and impact force, distribution of discharge fluxes at selected time intervals, 3D plot of sea state at

selected time intervals from different camera and light positions, and animation of tsunami propagation between source and target regions (Yalçıner *et al.,* 2006).

3.4. Creation of Tsunami Model Database

The initial process of the tsunami model studies is a compilation of the bathymetry data and tsunami source parameters, and identification of Numerical Gauge Points. In this section, the study domain is between the geographic coordinates of 27-42 E longitude and 38-48 N latitude, 30 arc-sec (~ 900 m) resolution bathymetry data of the Black Sea was obtained from the General Bathymetric Chart of the Oceans (GEBCO) with ASCII format. Data was gridded using Golden Software Surfer© (software application) and converted to *.grd format. Source files were created in NAMIDANCE with seismic source parameters of Bartın Earthquake was obtained from the existing literature (Alptekin, 1986). Table 3.4.1 shows information source parameters of the Bartın Earthquake. The duration of the simulation was chosen as 180 min and out put grid-files are produced at every 60 seconds. The major tsunami hydrodynamic parameters, such as maximum water surface elevations (positive tsunami amplitudes) at the Black Sea coasts were presented. In the Black Sea, the regions to be affected by tsunami were presented by calculating tsunami arriving time, generation and propagation of wave from the numerical simulation.

Table 3.4.1. September 3, 1968 of Bartın Earthquake source parameters (Alptekin, 1986).

Case	Mag.	Strike	Dip	Rake	L	W	Disp.	Focal Depth
Bartın Eq.	6.6 (Ms)	28°	38°	80°	25 km	12 km	1.5 m	4 km

3.5. Determination of the Numerical Gauge Points

Numerical Gauge Points are preselected coordinates in the coastal regions where the expected wave arrival times and amplitudes would be calculated. They were chosen from locations such as ports, marinas, coastal airports, and most populated regions. After numerical gauge points are defined, suggested offshore calculations performed with bathymetry depth levels ranging from zero to 15 meters obtained by Golden Software Surfer ©. Figure 3.5.1 shows locations and names of Numerical Gauge Points defined for 1939 and 1968 tsunami modeling. The two study areas (Bartın and Erzincan), coordinates and depths are shown in the Table 3.5.1.

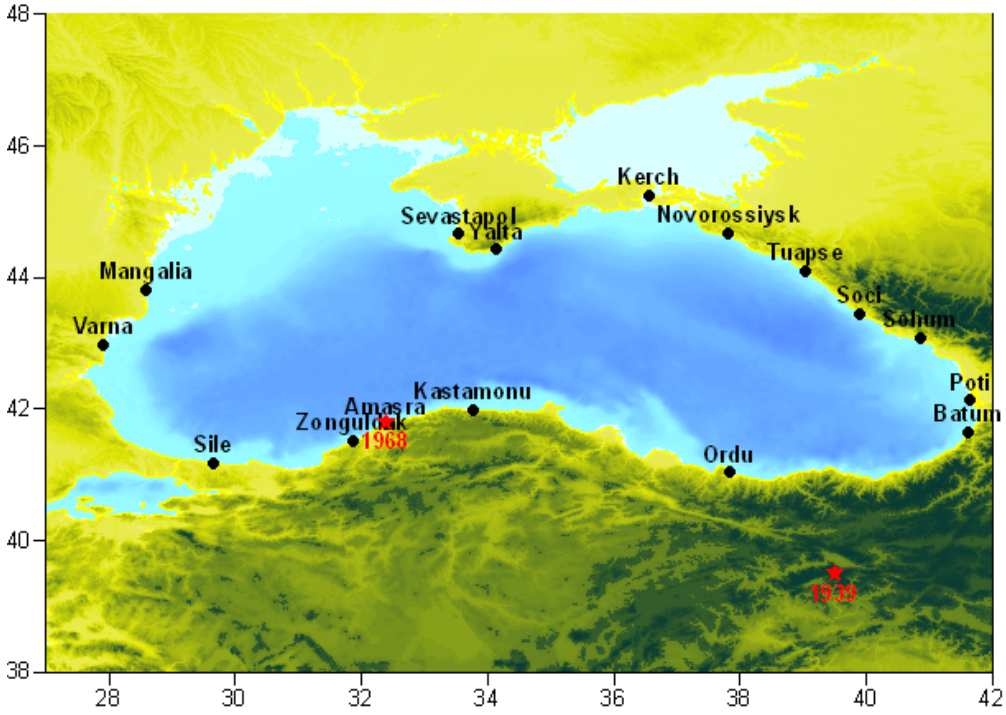

Figure 3.5.1. The distribution of Numerical Gauge Points defined for in these two focused events.

Table 3.5.1. Locations and bathymetry information for the selected Numerical Gauge Points in the study area.

No	Numerical Gauge Points	Lon	Lat	Depth (m)
1	Ordu	37.82626146°	41.03370391°	13
2	Kastamonu	33.77719791°	41.98903988°	1
3	Amasra	32.38318359°	41.76673554°	5
4	Zonguldak	31.86684682°	41.52020577°	6
5	Sile	29.63814637°	41.18162185°	3
6	Varna	27.90436184°	42.97058062°	0
7	Mangalia	28.58976684°	43.81355005°	2
8	Sevastapol	33.51884701°	44.49667406°	3
9	Yalta	34.10643016°	44.41906874°	13
10	Kerch	36.55566466°	45.24286788°	4
11	Novorossiysk	37.81823308°	44.66799088°	8
12	Tuapse	39.06208426°	44.0864745°	11
13	Soci	39.89245263°	43.453462°	3
14	Sohum	40.84828653°	43.07508782°	15
15	Poti	41.65103008°	42.13367395°	10
16	Batum	41.61311844°	41.65214717°	7

4. DESCRIPTION OF THE TSUNAMI EVENT AND NUMERICAL MODEL APPLICATION

4.1. Bartın Earthquake

The Bartın Earthquake occurred on 3 September 1968, at 08:19:52.2s and caused the Amasra Tsunami. Its surface magnitude was 6.6. The epicenter was located at the coordinates 41.8°N, 32.3°E. Location of the Bartın city and the epicenter of the earthquake can be seen in the Figure 4.1.1. Focal depth of the event was about 4 km (Alptekin, *et al.,* 1986). Although it is an intermediate size earthquake, the Bartın Earthquake caused some casualties and considerable damage in the towns of Bartın and Amasra and other villages in northwestern Turkey. 24 persons died, 2498 houses were partly destroyed (Lander *et al.,* 1969). It had even been noticed in the cities like Ankara, Bursa, Istanbul and Samsun. According to the inhabitants, sea level in the Big Port drew back 1.5 m then risen 3 m afterwards and flooded the houses and restaurants. Damage was generally severe in almost all the villages in the Çakraz Valley. Wedding (1968) stated that the sea inundated 100 m in Amasra and after 14 minutes the second wave inundated the shore about 50-60 m. The intensity of this tsunami can be considered as III–V according to the new tsunami intensity scale of Papadopoulos and Imamura (2001). Within the epicenter region, cracks in the alluvial ground, several landslides on the steeper slopes were observed. Isoseismal maps were prepared for Bartın Earthquake (Albers and Kalafatçıoğlu, 1969: Ergünay and Tabban, 1983). The isoseismal map of the Bartın Earthquake is shown in Figure 4.1.2. During this earthquake, the precipitous coastline between Amasra and Çakraz uplifted. This uplifting estimated by Ketin and Abdüsselamoğlu (1970) to be 35–40 cm, lowered the sea level on the coastal rock, resulting in the appearance of mussels and moss. Lander (1969) reported that the sea receded 12 to 15 m in Çakraz at the onset of the earthquake and never returned entirely to its original level. This wave dragged many objects and caused many boats to be stranded. The reason for this progression was most probably the uplifting around Çakraz. Alptekin *et al.* (1986) with the help of the modelling of P and SH waves, concluded that the event was caused by thrust faulting with fault parameters of 28° strike, 38° dip and 80° rake. They also suggested that the Bartın Earthquake provided the

first seismological evidence for active thrust faulting at the southern margin of the Black Sea.

Figure 4.1.1 Location of the Bartın city (Image provided by the internet, http://www.cografya.gen.tr/tr/bartin).

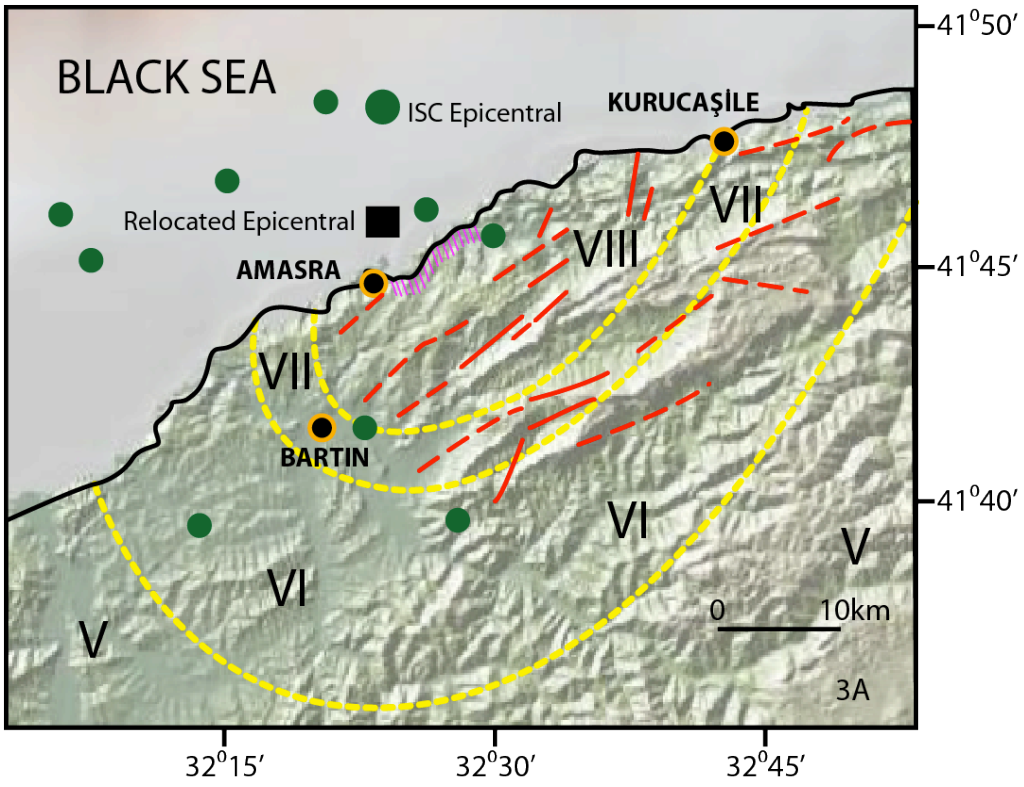

Figure 4.1.2. Isoseismal map of the Bartın Earthquake (reproduced from Ergünay ve Tabban, 1983).

Isoseismals are shown by yellow broken lines (Ergünay and Tabban, 1983). The big green circle and black square denote the epicenters proposed by ISC and Alptekin *et al.* (1986). The ISC epicenter for the main shock was located in the Black Sea, about 10 km north of Amasra. Small green dots represent the ISC-determined epicenters of aftershocks. The purple shaded area indicates the location of the coastal uplift observed by Ketin and Abdüsselamoğlu (1970). Thin red dashed or continuous lines show faults (Ketin and Abdüsselamoğlu, 1970). Contours are isoseismal lines enclosing areas of varying intensities according to the Mercalli-Sieberg scale (Roman numerals indicate intensities).

4.2. Investigation of Hydrodynamic Parameters of Amasra Tsunami

In order to compute the tsunami hydrodynamic parameters, tsunami simulation was performed. The model created the initial wave by using tsunamigenic rupture parameters of the earthquake. The location of tsunami initial wave is seen in the Figure 4.2.1. The time

histories of water level fluctuations at the numerical gauge points were obtained (Figure 4.2.2).

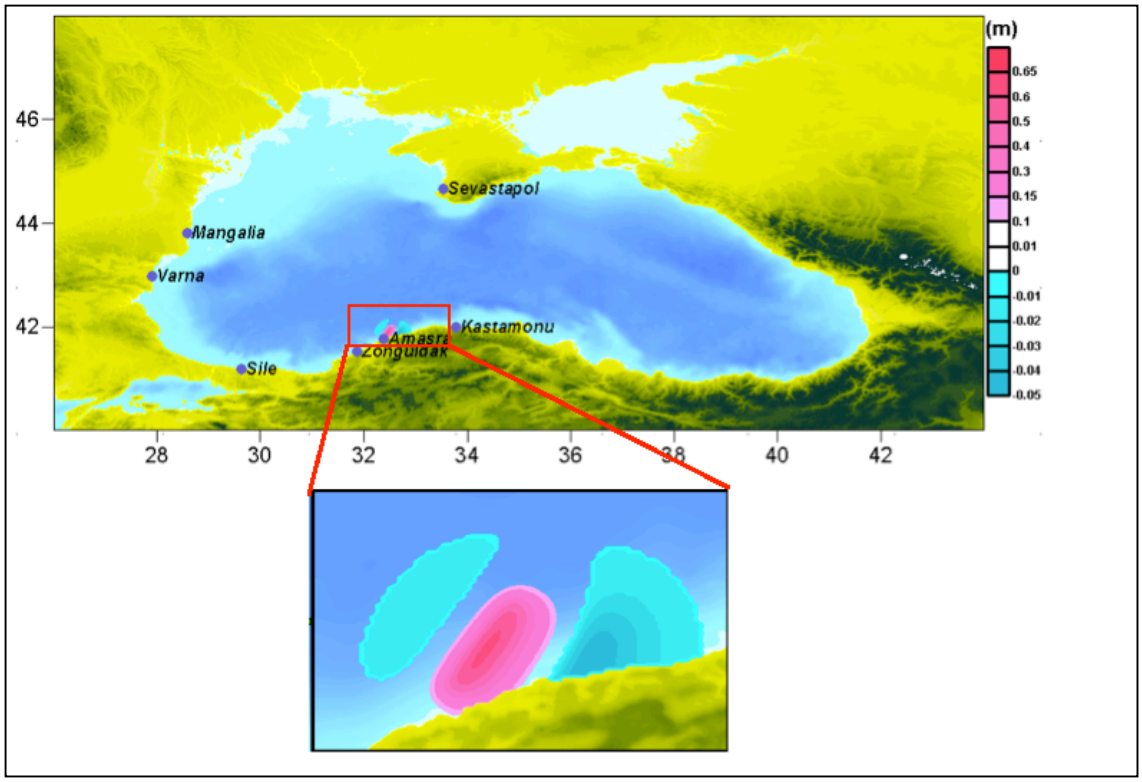

Figure 4.2.1. Initial tsunami source and some of the numerical gauge points are seen on the map. Water surface elevation is in meter. Source can be seen in the zoom area.

Arrival time of the wave and wave amplification were investigated to check the propagation of wave characteristics along the path in the sea and near the shore shown with names of places. Computed water surface elevations at the shore and near the shore are seen in the Figure 4.2.2.

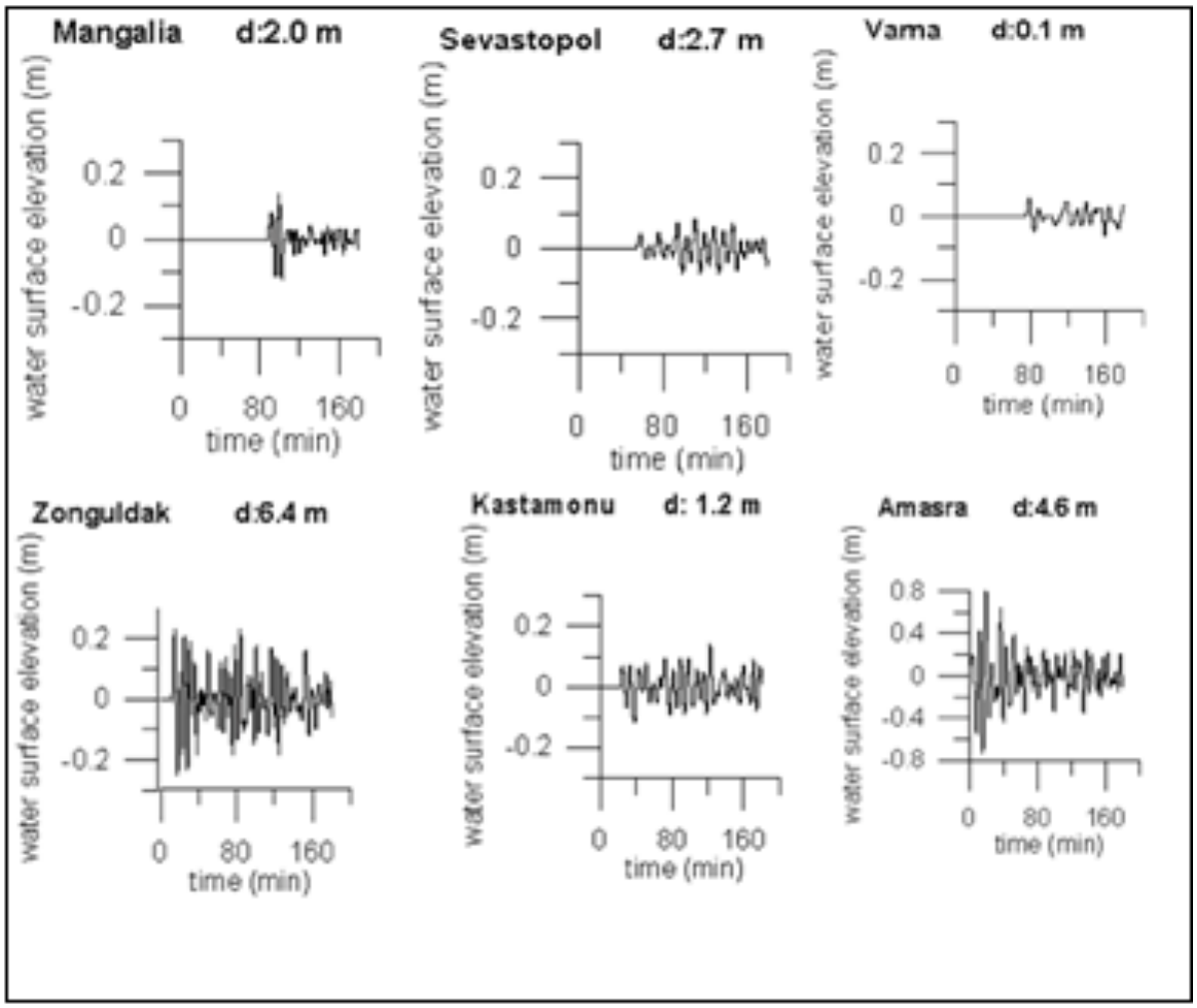

Figure 4.2.2. Comparison of synthetic tsunami records at numerical gauge points. The vertical scale shows water surface elevation (wse) in meters and horizontal scale shows time (t) in minutes, d is the bathymetry depth level range in meters.

From the model studies, arrival time of initial wave and maximum wave in minutes and maximum positive and negative wave amplitudes were observed. Summary of results based on the selected points are shown in the Table 4.2.1.

Table 4.2.1. Summary results of model study are seen for Amasra Tsunami triggerred by the Bartın Earthquake.

Name of Numerical gauge pt.	**Depth of N. gauge pt. (m)**	**Arrival time of initial wave (min)**	**Arrival time of max. wave (min)**	**Maximum (+) amp. (m)**	**Maximum (-) amp. (m)**
Kastamonu	1	22.20	122.87	0.14	-0.12
Amasra	**5**	**0.00**	**19.43**	**0.80**	**-0.73**
Zonguldak	6	12.13	14.53	0.23	-0.25
Sile	3	42.87	95.33	0.15	-0.10
Varna	0	75.20	78.17	0.06	-0.06
Mangalia	2	88.33	98.57	0.14	-0.12
Sevastopol	3	55.60	110.33	0.08	-0.07
Soci	4	77.70	107.60	0.02	-0.02

Graphical demonstration of the arrival time of the initial wave and maximum positive amplitude are shown in the Figure 4.2.3 and Figure 4.2.4, respectively. As a result, arrival times for Kastamonu, Sevastapol, Varna, are 22, 55 and 75 minutes, respectively. The uplift of the water surface of the initial wave is 0.80 meters (Figure 4.2.3). The amplitude of tsunami does not exceed 0.2 meters in almost all other gauge points.

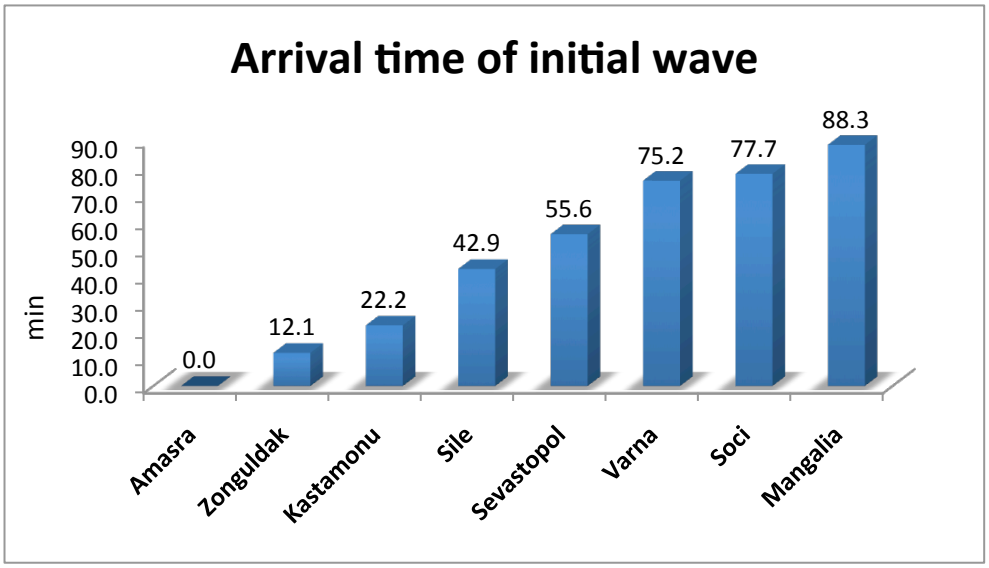

Figure 4.2.3. Arrival time of initial wave at the numerical gauge points.

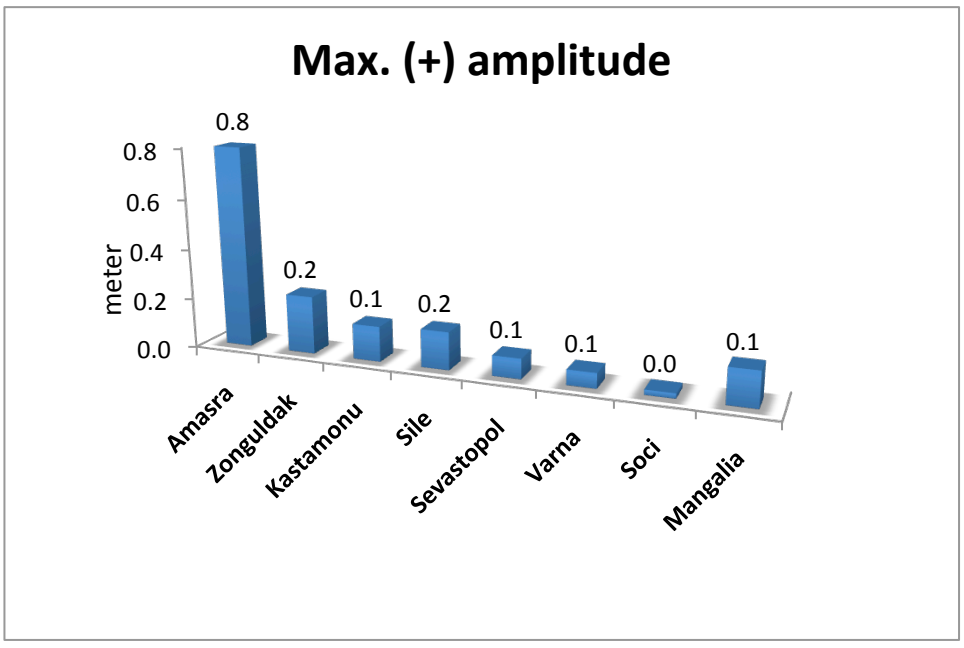

Figure 4.2.4. Maximum positive amplitude of the tsunami wave at the numerical gauge points.

The distributions of the computed maximum elevations of the sea level (tsunami directivity) in the sea and along the north and south coasts were obtained by three hours numerical simulation. Figure 4.2.5 shows the distribution of tsunami energy.

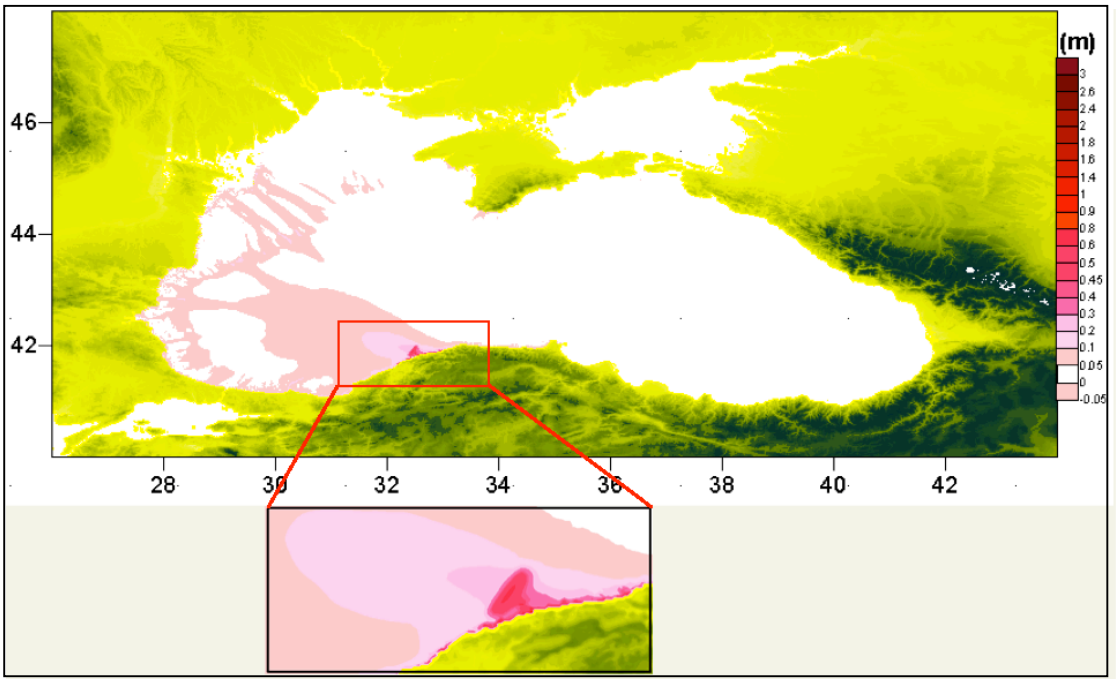

Figure 4.2.5. Distribution of tsunami energy (directivity).

In this study, snapshots of the tsunami wave propagation time intervals corresponding to 10, 30, 60 minute scenarios were performed by the numerical simulation. Figure 4.2.6 shows these snapshots for the 1968 Bartın event. The effects of tsunami waves are clearly visible when synthetic tsunami simulations at 10, 30, and 60 minute are compared. The water surface height scale is given in meters.

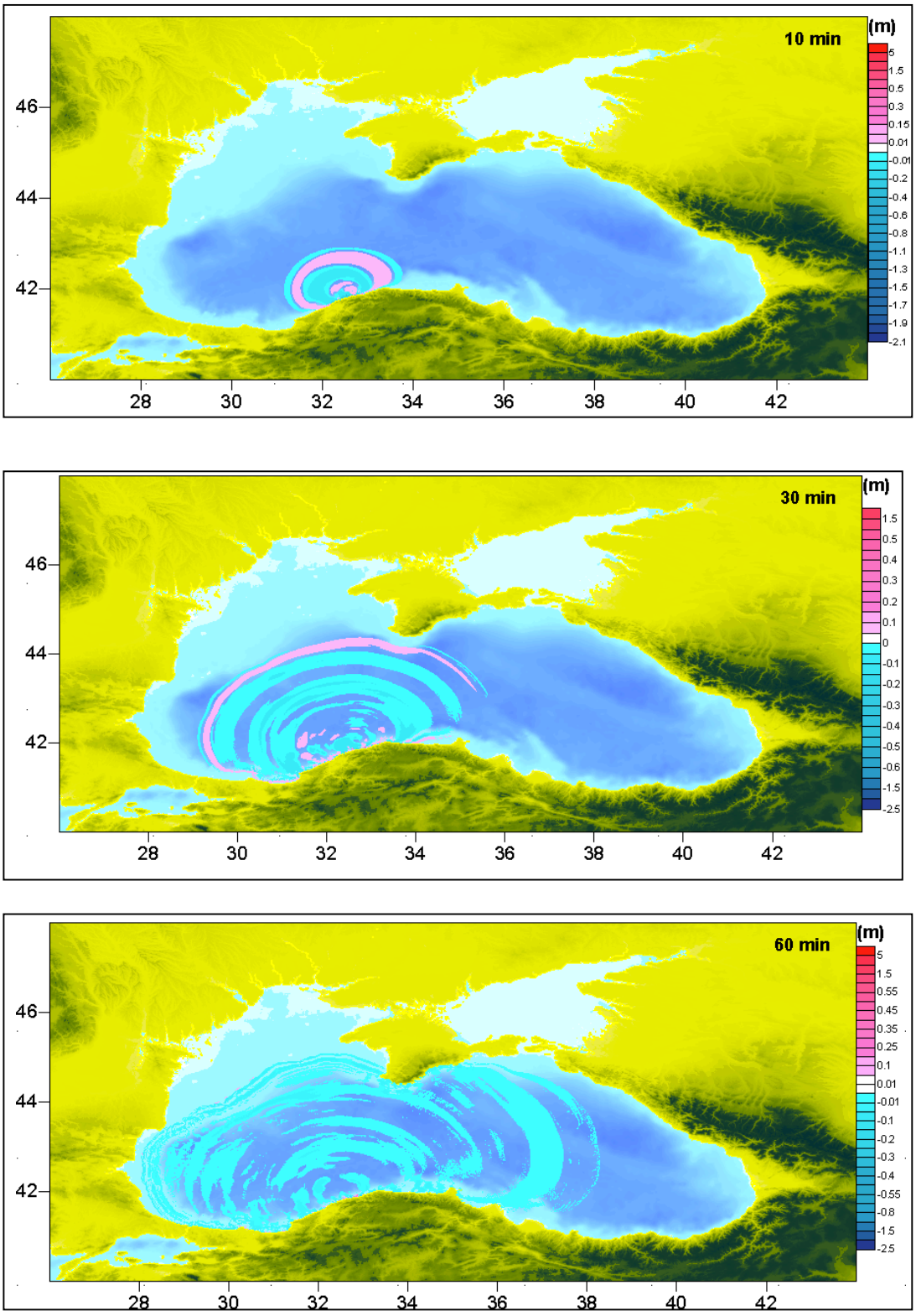

Figure 4.2.6. Sea state at the time of 10, 30 and 60 minutes.

4.3. Erzincan Earthquake

The Erzincan Earthquake occurred on 26 December 1939 at 23:57 (GMT) and triggered the Fatsa Tsunami. Its surface magnitude was 8. The epicenter was located at the coordinates 39.80N-39.51E with focal depth about 20 km (KOERI database). Location of the Erzincan city and the epicenter of the earthquake can be seen in the Figure 4.3.1. Intensity was 11–12 (Nikonov, 1997). The earthquake was felt over a very large area (Amasya, Tokat, Sivas, Kırşehir, Ankara, Çankırı, Kayseri, Samsun, Ordu) (Altınok, 2000). It was probably one of the most destructive earthquakes and more than 40,000 people lost their lives and some 12,000 houses were destroyed in an area of 400 km by 120 km. The right-lateral strike-slip rupture had a length of approximately 350 km and associated slip was 4 m. An iso-seismal map of this earthquake is shown in Figure 4.3.2. Figure 4.3.3 indicates the damage caused by the 1939 Earthquake. The contemporary importance of the NAFZ was first noticed with the occurrence of the 1939 Erzincan Earthquake (Pamir and Ketin, 1941 and Parejas *et al.,* 1942). This fault is an active right-lateral strike-slip fault (Ketin, 1948). The 1939 Earthquake greatly contributed to a fuller understanding of the NAFZ (Figure 4.3.4).

Figure 4.3.1. Location of the Erzincan city (image provided by the internet, http://en.wikipedia.org/wiki/File:Erzincan_map.gif).

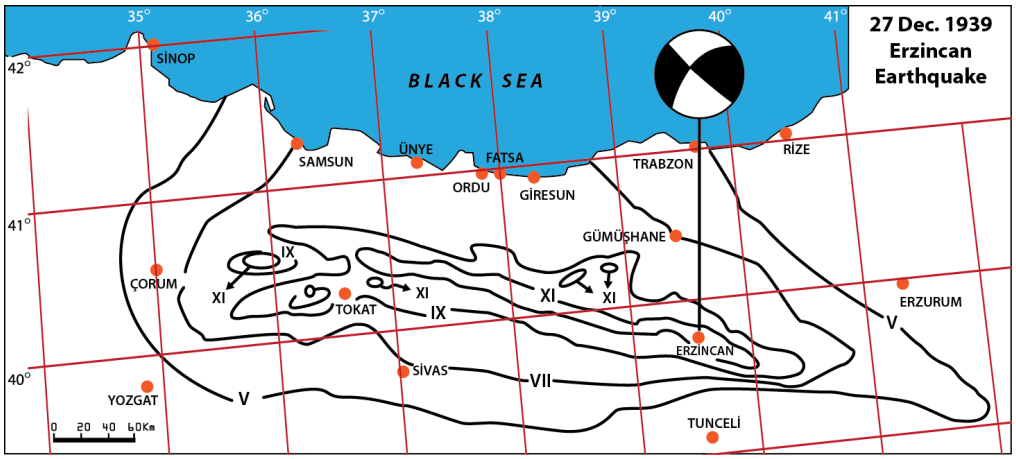

Figure 4.3.2. Isoseismal map of the Erzincan Earthquake, modified from Pamir and Ketin, (1941). The authors have used the MS Scale. Focal mechanism solution indicates strike slip faulting (McKenzie *et al.,* 1972).

Figure 4.3.3. Historical photographs around Erzincan (Image provided by the internet, http://mimoza.marmara.edu.tr/~avni/ERZiNCAN/deprem/askeriokul/2.htm).

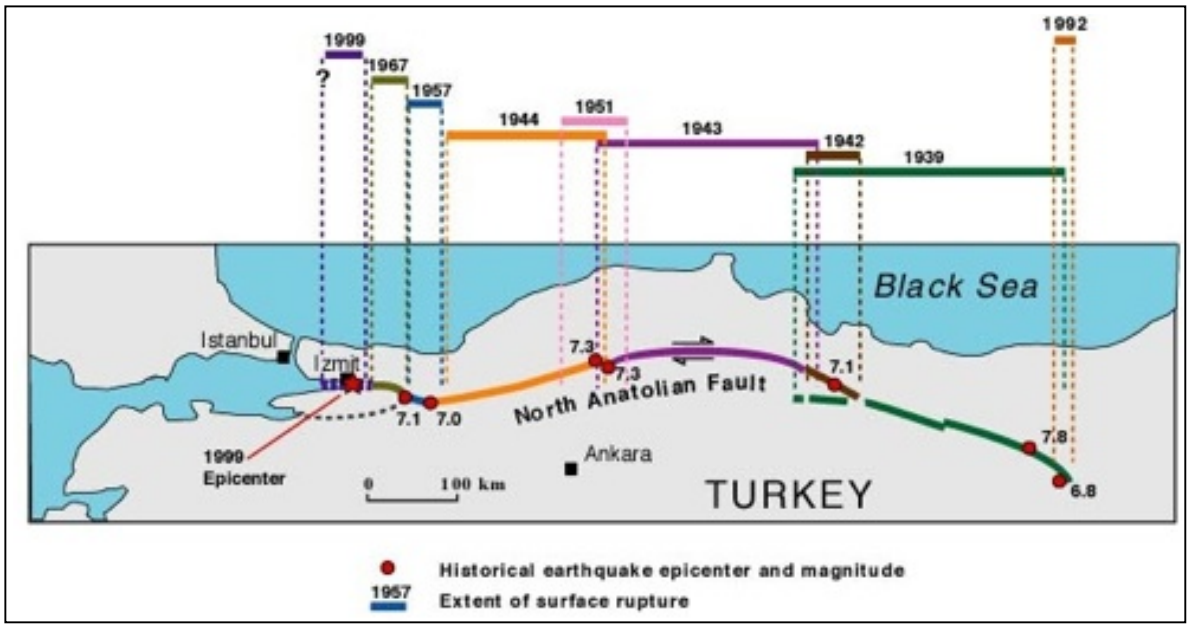

Figure 4.3.4. A map of Turkey showing the North Anatolian fault and the successive earthquakes rupturing the fault starting from the east in 1939 (Image provided by the USGS).

Tsunami waves were observed and recorded in the Black Sea after the great earthquake. The sea receded 50 m Fatsa and Giresun, and after that advanced 20 m near Fatsa town. In the Ordu, the people at the harbor witnessed that the sea initially was calm, then receded ~ 15 m, and returned its original position in 5–10 min (Altınok and Ersoy, 2000). Parejas *et al.* (1942) mentioned that a person in Fatsa wanted to dive into the sea instinctively at the time of the earthquake, but he was not able to reach the sea because it had receded about 50 m. After a while, when the sea came back, the edge of the coast advanced 20 m. The sea receded 100 m during the earthquake in Ünye. Tsunami amplitudes were smaller on the Russian coasts than in Turkey. The initial rise in the sea level was recorded at six tidal stations on the northern coast of the Black Sea.

4.4. Investigation of Hydrodynamic Parameters of Fatsa Tsunami

In order to compute the tsunami hydrodynamic parameters, tsunami simulation was performed for the second case. Epicenter of the 1939 event is ~ 60 km away from the south coast of the Black Sea. Figure 4.4.1 shows the epicenter location of the event. Source parameters of Erzincan Earthquake (Ms=8.0, on 26 December 1939) compiled by Doğan Kalafat , 2005 (Table 4.4.1).

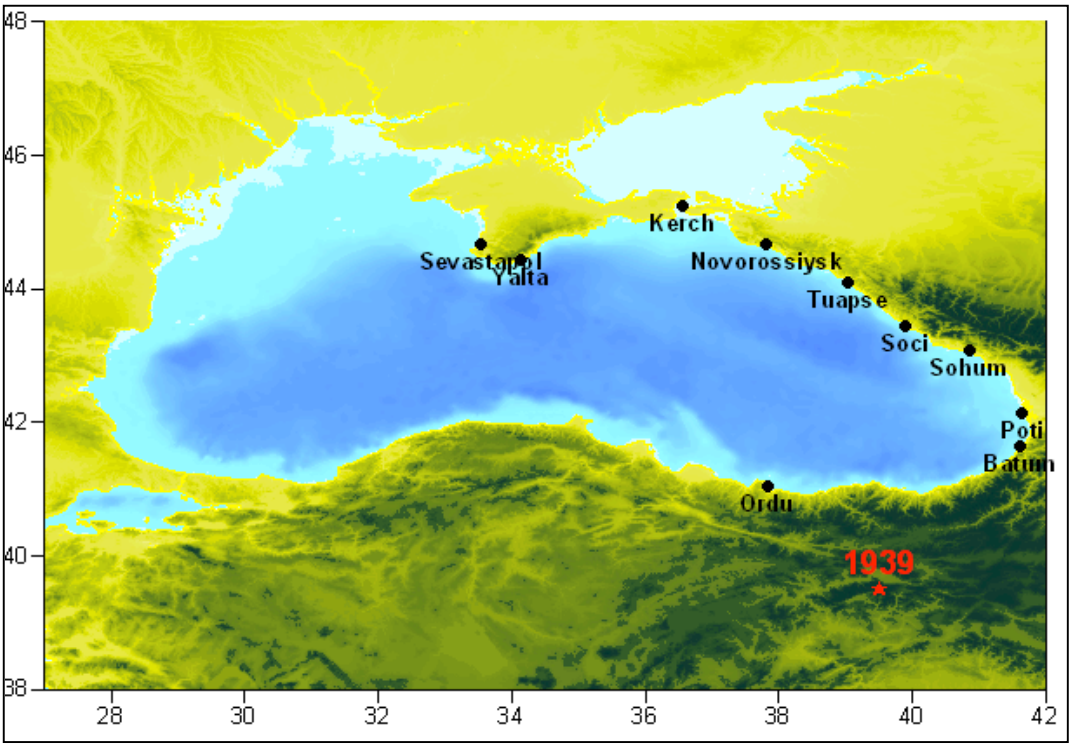

Figure 4.4.1. Epicenter of Erzincan Earthquake and some of the selected numerical gauge points are seen on the map.

Table 4.4.1 26 December 1939, Erzincan Earthquake fault parameters, (Kalafat *et al.,* 2005).

Fault Parameters	
Epicenter of Earthquake	39.5E, 39.80 N
Fault Length	350 km
Strike	200°
Rake	110°
Dip	60°
Focal Depth	20 km

Since the Erzincan Earthquake occurred on land, it couldn't have generated a tsunami directly. However, the Fatsa Tsunami may be originated by a secondary faulting, or a variety of sea-floor landslides referenced in the publications (Kuran and Yalçıner, 1993; Pelinovsky, 1999). There are not any sufficient data to determine the location and mechanism of tsunami source. Yalçıner *et al.* (2004) reported about 30 cm wave amplitude was observed between Ordu and Ünye cities based on the eyewitness of the people living in the area. In terms of the available reports from an indigenous people, source of the tsunami is likely to happen in that area. In this region, a tsunami source model was established in the Fatsa region. Many scenarios applied to investigate a possibility of landslide triggered that tsunami. The outcomes of scenarios were compared with previously existing tide gauge records from the northern part of the Black Sea, thought to be from the Fatsa Tsunami (Figure 4.4.2).

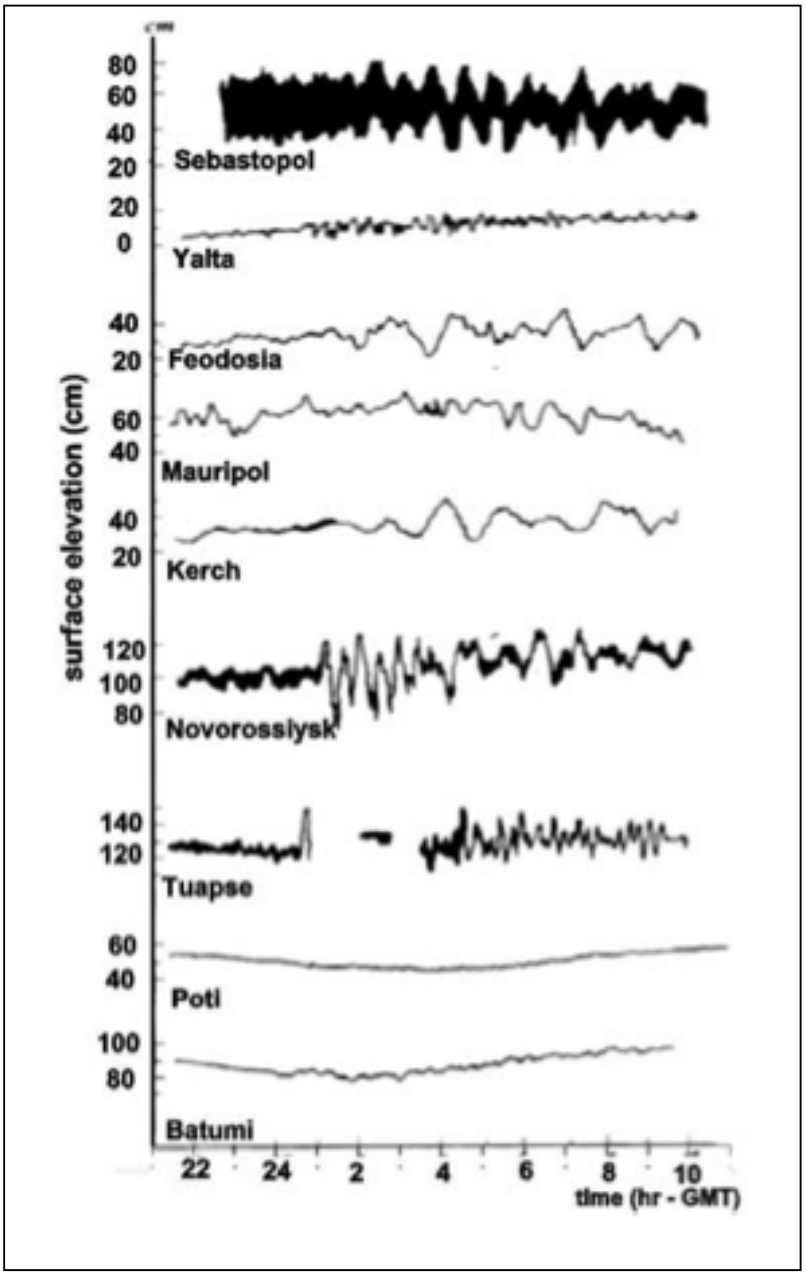

Figure 4.4.2. The instrumental records of water surface fluctuations at the tide-gauge stations for the1939 event.

In the light of the available reports from local people and based on the recorded Novorossysk water surface fluctuations, some tsunami source scenarios applied and results were compared. Firstly, major and minor axes variation compared with same wave amplitude values and then wave amplitude variation compared with same major and minor axes values (Table 4.4.2). Until best compatible results were obtained, simulation scenarios

were run.

Table 4.4.2. Major and minor axes variation compared with same wave amplitude values and wave amplitude variation compared with same major and minor axes values.

2 m Wave Amplitude		
Major and Minor Axes Length	**Arrival time of initial wave (min)**	**Max. wave amplitude(m)**
12km-6km	50.85	0.35
10km-8km	50.55	0.27
10km-6km	50.95	0.31
8km-6km	51.05	0.26
Same Size Major and Minor Axes Length (12km-6km)		
Wave amplitude	**Arrival time of initial wave (min)**	**Max. wave amplitude(m)**
1m	51.65	0.19
2m	50.85	0.35
4m	50.55	0.63

According to modeling results, water surface elevation a little bit increases when major axis mass increases for the same wave amplitude forced. The water surface elevation increases when wave amplitude increases for the same axes forced.

As seen in the Figure 4.4.3 and Figure 4.4.4; 2 m wave amplitude with 12 km-6 km major and minor axes is the best prediction that fits the recorded real data at Novorossysk with arrival of initial wave.

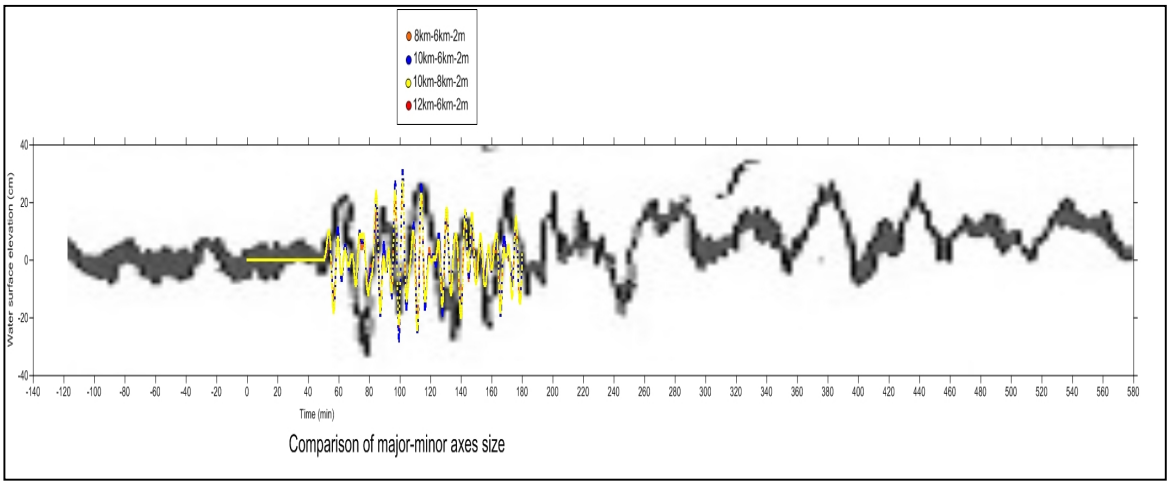

Figure 4.4.3. Comparison of major-minor axes size.

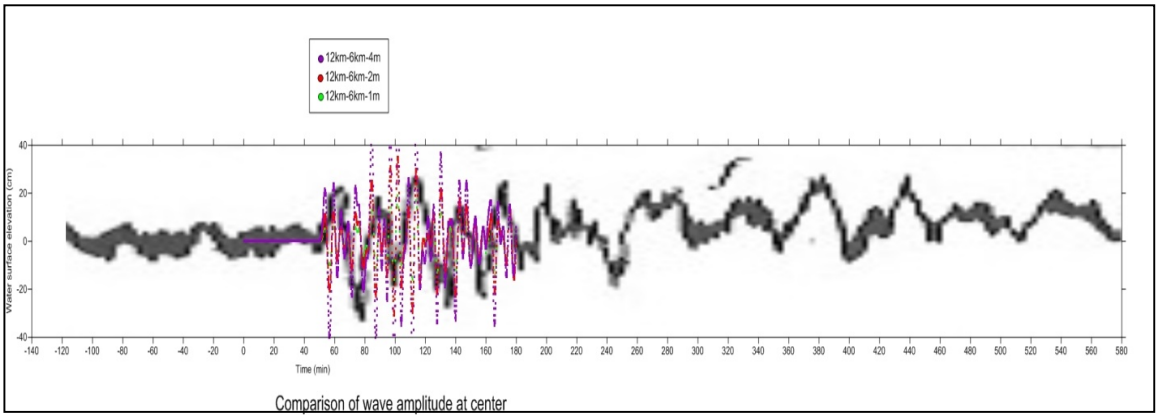

Figure 4.4.4. Comparison of wave amplitude at center.

Based on the scenarios; the tsunami source was selected as 2 m positive amplitude and -2 m negative amplitude with length of major axis 12 km and length of minor axis 6 km of sliding mass (Figure 4.4.5).

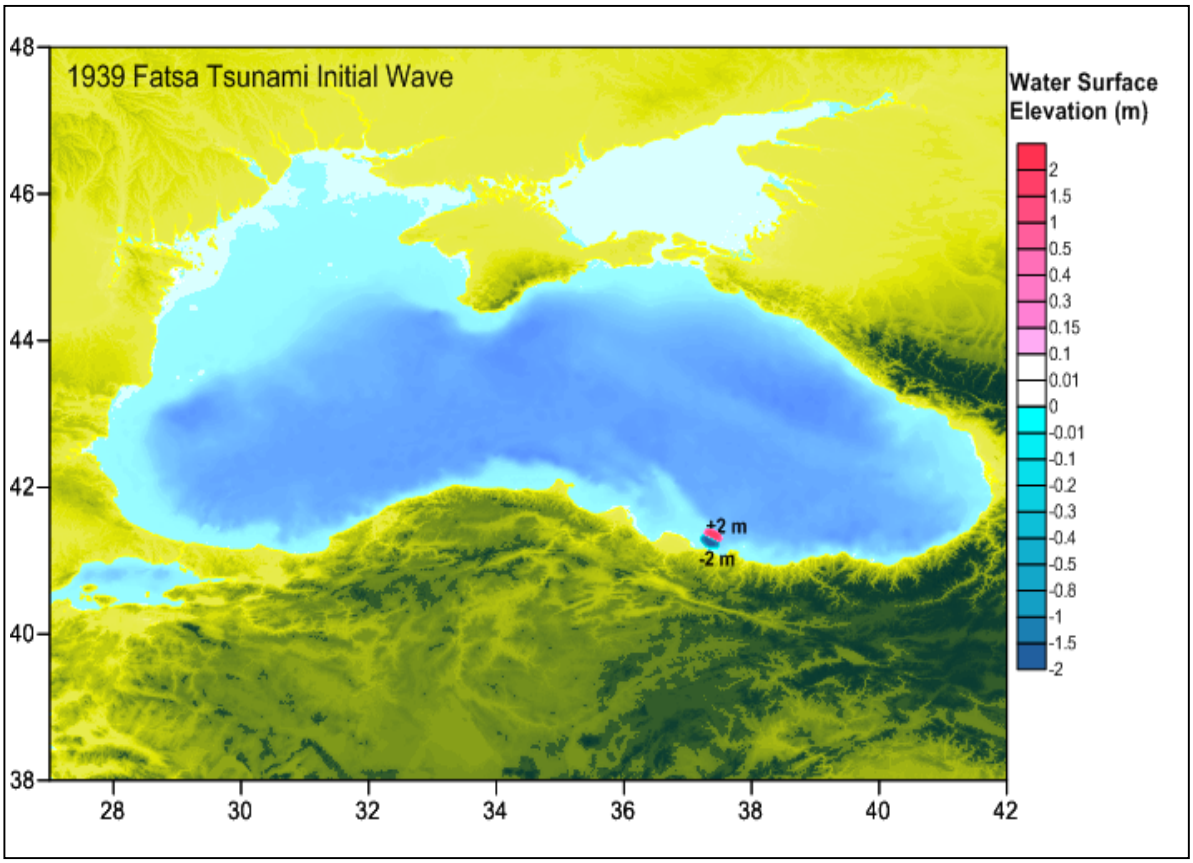

Figure 4.4.5. Location of the tsunami source and initial wave of Fatsa Tsunami were shown.

As it can be seen in the Figure 4.4.5, positive amplitude of the tsunami wave is in the offshore side because the leading elevation wave is observed at Novorossiysk and other locations in the Northern Black Sea. The initial tsunami source is seen on the map. Water surface elevation is in meters. Figure 4.4.6 shows the distribution of tsunami energy. In this study, snapshots of the tsunami wave propagation time intervals corresponding to 10, 30, 60 minute scenarios were performed by the numerical simulation. Figure 4.4.7 shows these snapshots for the 1939 Erzincan Earthquake.

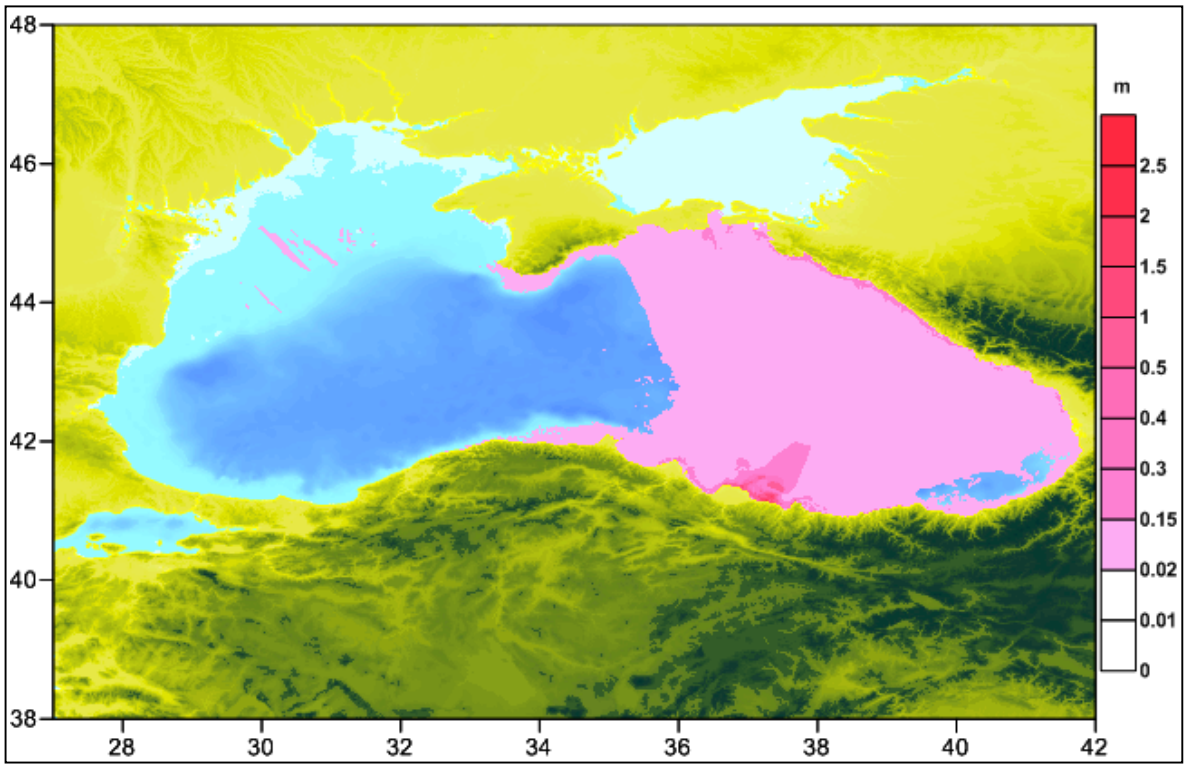

Figure 4.4.6. Distribution of tsunami energy (directivity).

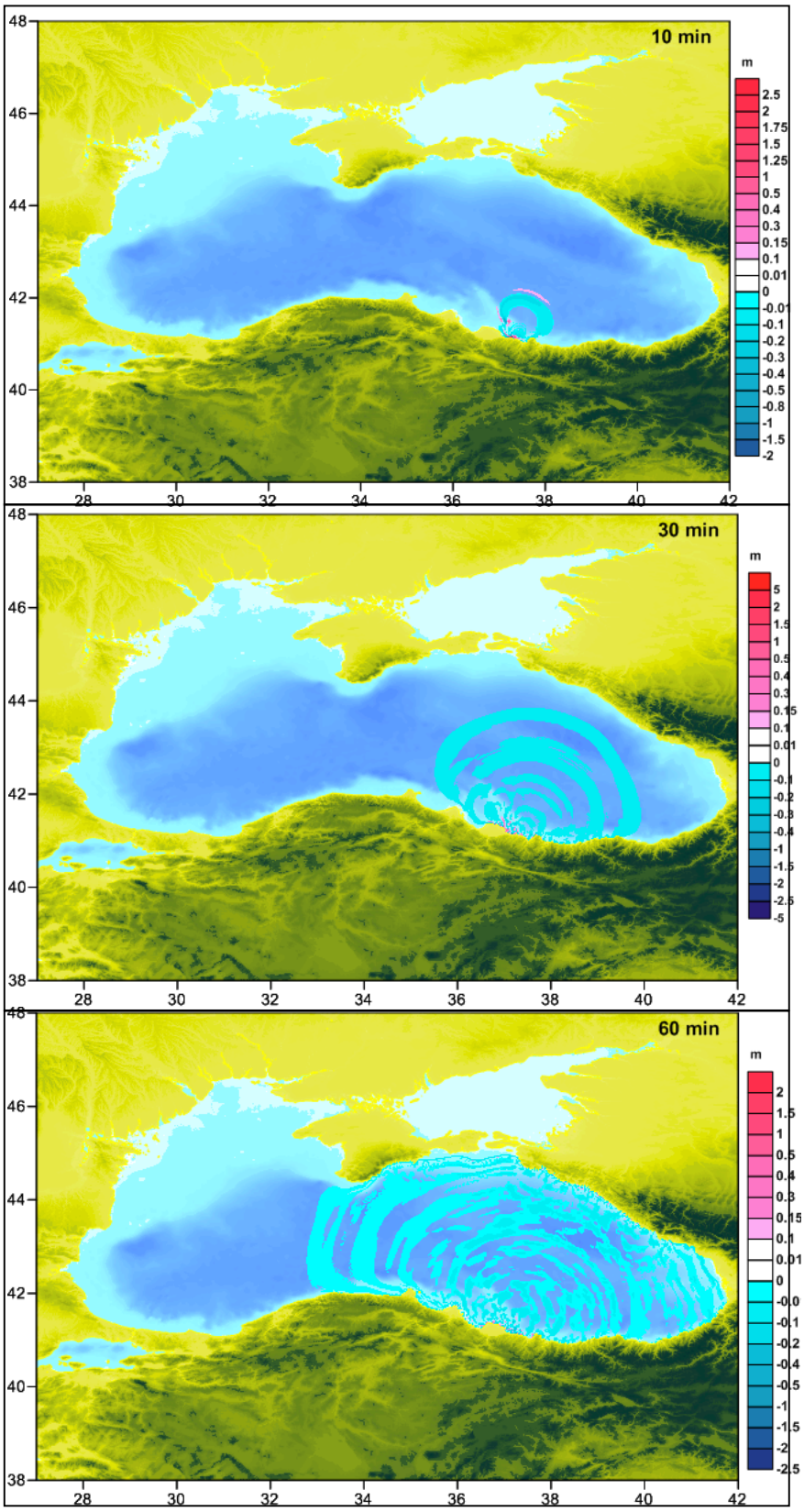

Figure 4.4.7. Sea state at the time of 10, 30 and 60 minutes.

In this thesis study, the next step was to compare instrumental records with numerical simulation results. The locations of the points for 1939 event could be seen in the Figure 4.4.8. As a result of Fatsa numerical tsunami modeling, Table 4.4.3 gives the distribution of maximum positive amplitude and arrival time of waves according to the numerical gauge points.

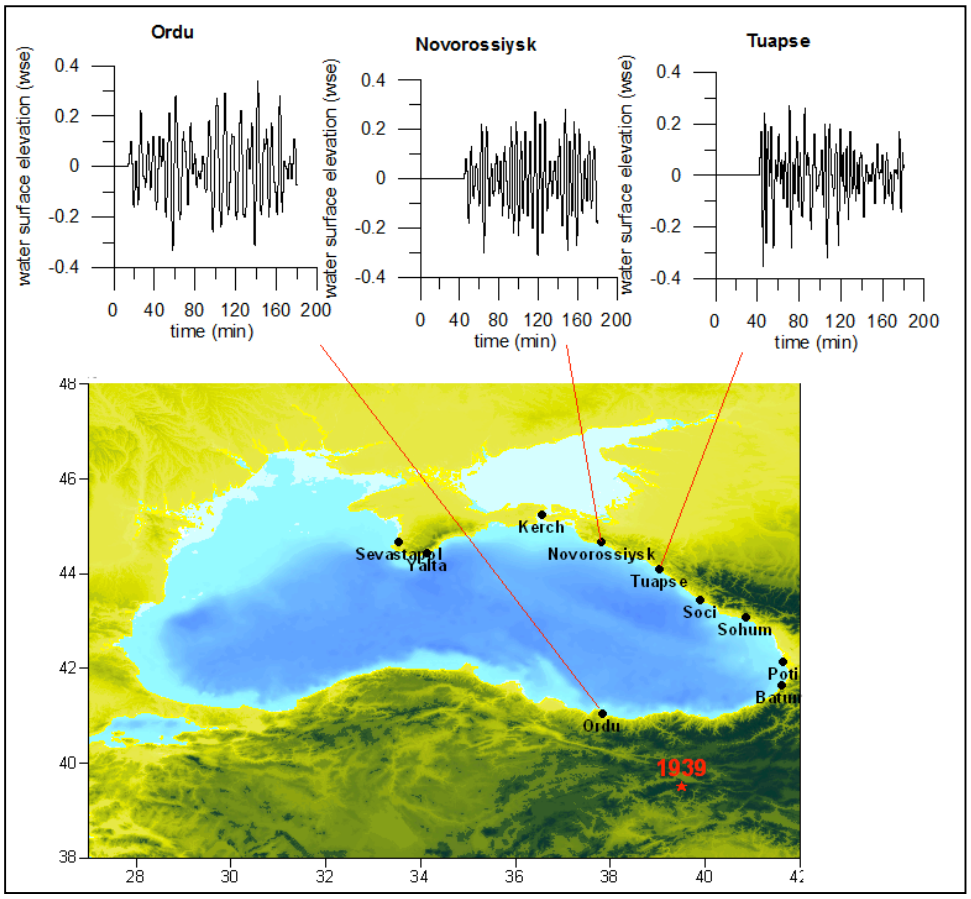

Figure 4.4.8. Some numerical gauge points for 1939 Fatsa Tsunami simulation model.

Table 4.4.3. Summary results of the tsunami numerical model.

Name of Gauge Points	Depths of Gauge Points (m)	Arrival time of initial wave (min)	Arrival time of max. wave (min)	Max. (+) amp. (m)	Max. (-) amp. 8m)
ORDU	**13**	**14.95**	**26.55**	**0.58**	**-0.6**
YALTA	**13**	**57.45**	**120.35**	**0.14**	**-0.23**
KERCH	**4**	**116.35**	**140.45**	**0.06**	**-0.05**
NOVOROSSIYSK	**8**	**50.85**	**101.55**	**0.35**	**-0.31**
TUAPSE	**11**	**46.15**	**59.05**	**0.7**	**-0.66**
POTI	**10**	**53.05**	**112.15**	**0.35**	**-0.34**
BATUM	**7**	**49.65**	**126.85**	**0.25**	**-0.29**
SOCI	**3**	**40.45**	**63.55**	**0.57**	**-0.41**
SOHUM	**15**	**52.95**	**86.55**	**0.32**	**-0.3**

5. DIGITIZATION OF THE TIDE GAUGE DATA

Maximal tsunami waves related the 1939, Erzincan event was recorded by the tide gauges in the Northern Black Sea coast of Sebastopol, Yalta, Feodosia, Mariupol, Kerch, Novorossiysk, Tuapse, Poti, Batum towns that are helpful for comparison with numerical results for several coastal locations. The records from the north of the Black Sea were digitized using TESEO (Turn the Eldest Seismograms into the Electronic Original Ones) produced by Pintore *et al.* (2005).

TESEO is produced to convert seismic traces on the paper to a digital series of seismic ground motion for the usage of present waveform analysis tool (Battllo, 2008). Using these programs, it is possible to pick the points that represent the seismic waveform. It is the plug-in of powerful graphics software named GIMP supports very high-resolution images as scanned historical seismograms. However, during digitization process could be encountered some problems due to paper quality and resolution of records and mechanism of seismograms (Başarır, 2011). As seen in the Figure 5.1, the waveform has thick traces that make difficult to digitize correctly the frequency path on record. Figure 5.2 shows another example that is impossible to perform digitizing.

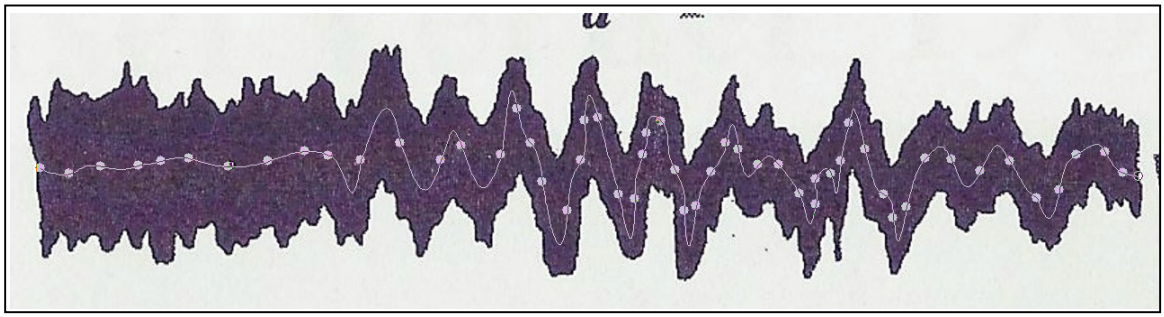

Figure 5.1. The record of tsunami waves in Sevastopol.

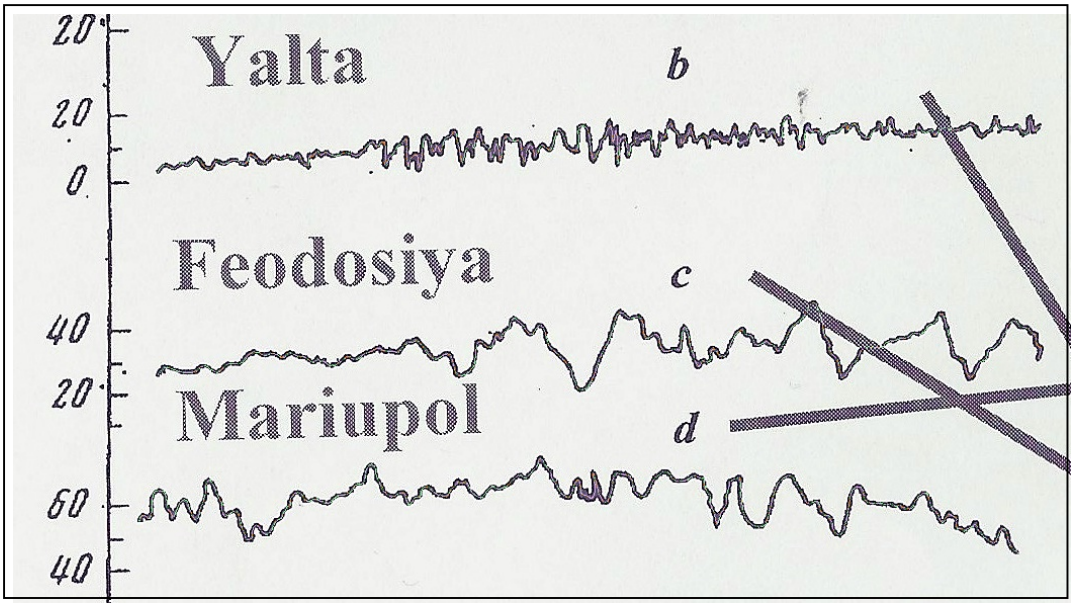

Figure 5.2. The heights of tsunami waves in Yalta, Feodosiya, Mariupol cities.

Since the historical records were exposed to many external factors, it is possible to see erased parts of traces or interrupted trace lines. Another difficulty during digitization process is the interruptions on the trace lines (Figure 5.3).

Figure 5.3. The record of tsunami waves for Tuapse.

In this study, instrumental records from Kerch, Novorossiysk, Tuapse, Poti, and Batum cities were digitized (Figure 5.4).

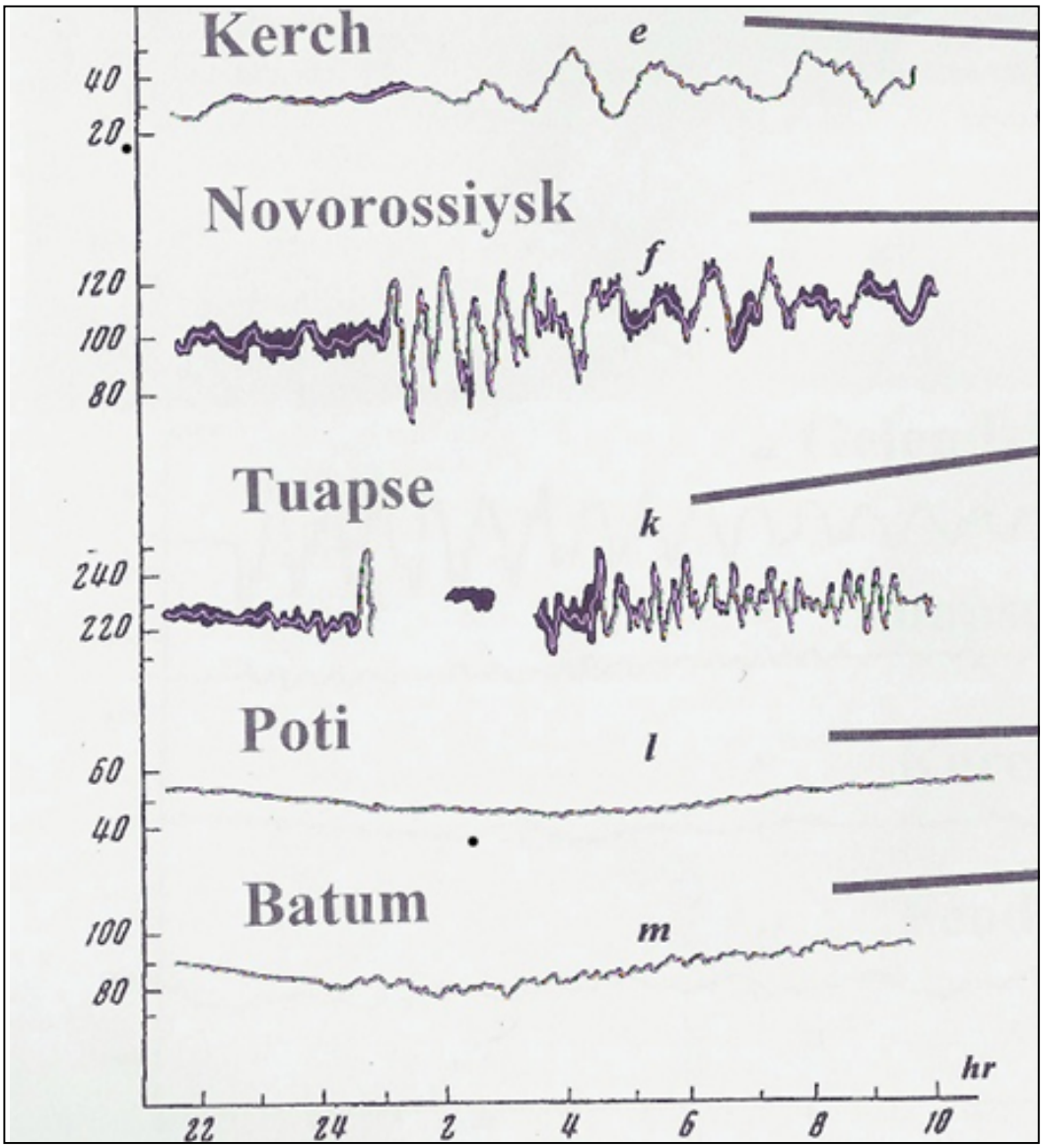

Figure 5.4. Mareogram records were digitized for Kerch, Novorossiysk, Tuapse, Poti, Batum, respectively. X axis is time in minutes, y axis is height in cm.

Figure 5.5.1, Figure 5.5.2, Figure 5.5.3, Figure 5.5.4 show graphical demonstrations of digitized wave traces obtained by Matlab program and comparison with instrumental records. X axis is time in hours, y axis is height in cm.

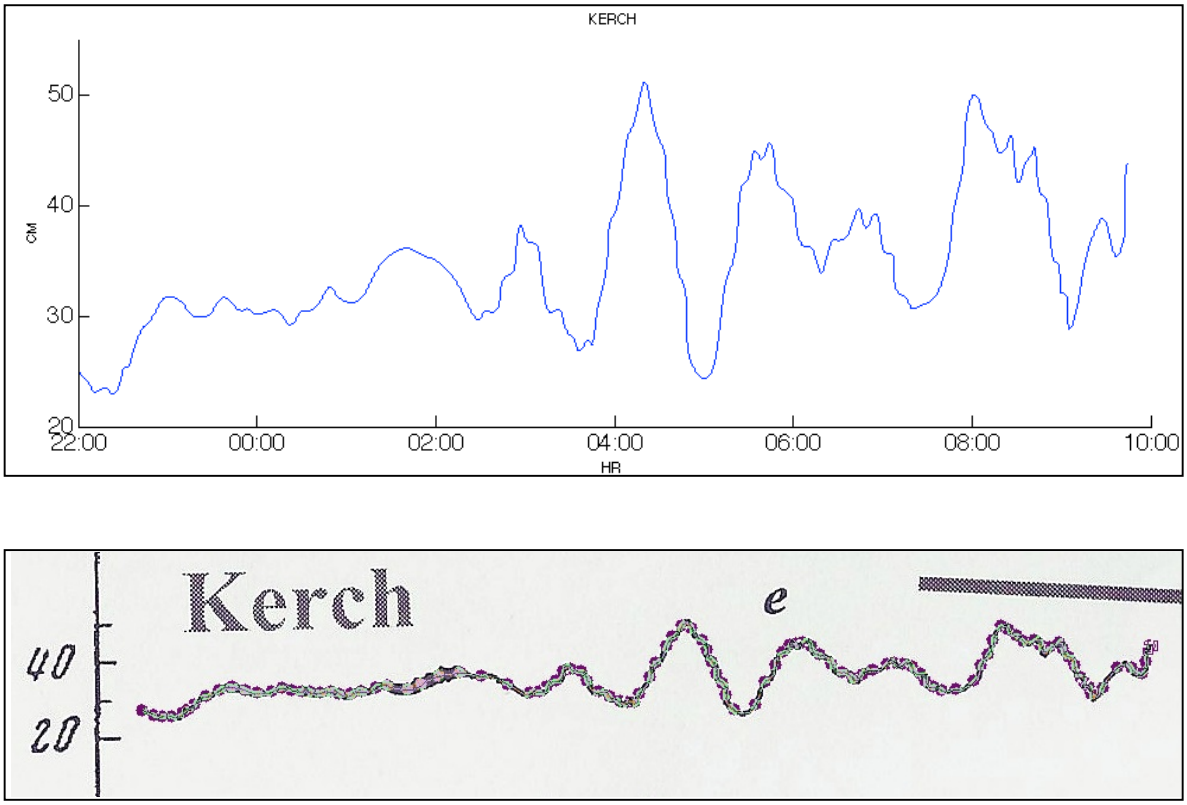

Figure 5.5.1. Kerch digitized wave trace (above) and instrumental record (bottom).

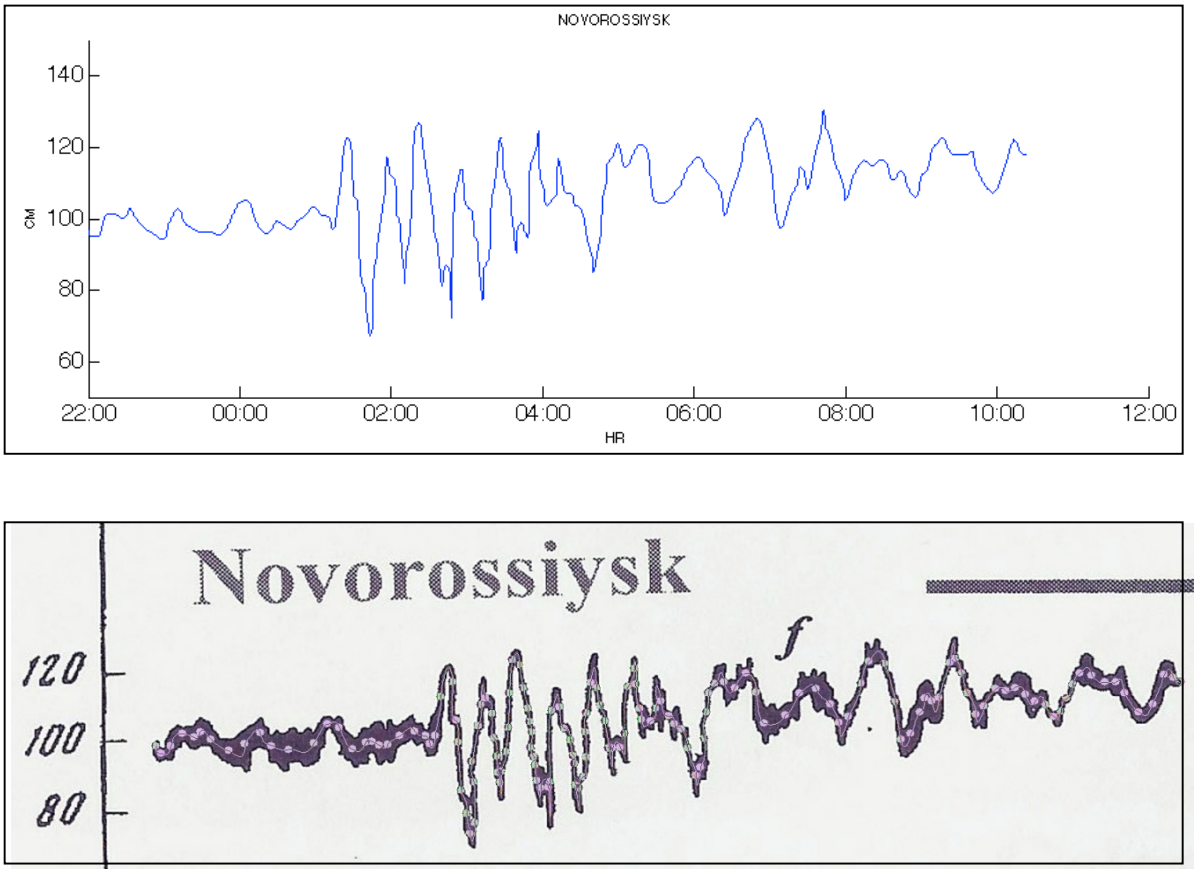

Figure 5.5.2. Novorossiysk digitized wave trace (above) and instrumental record (bottom).

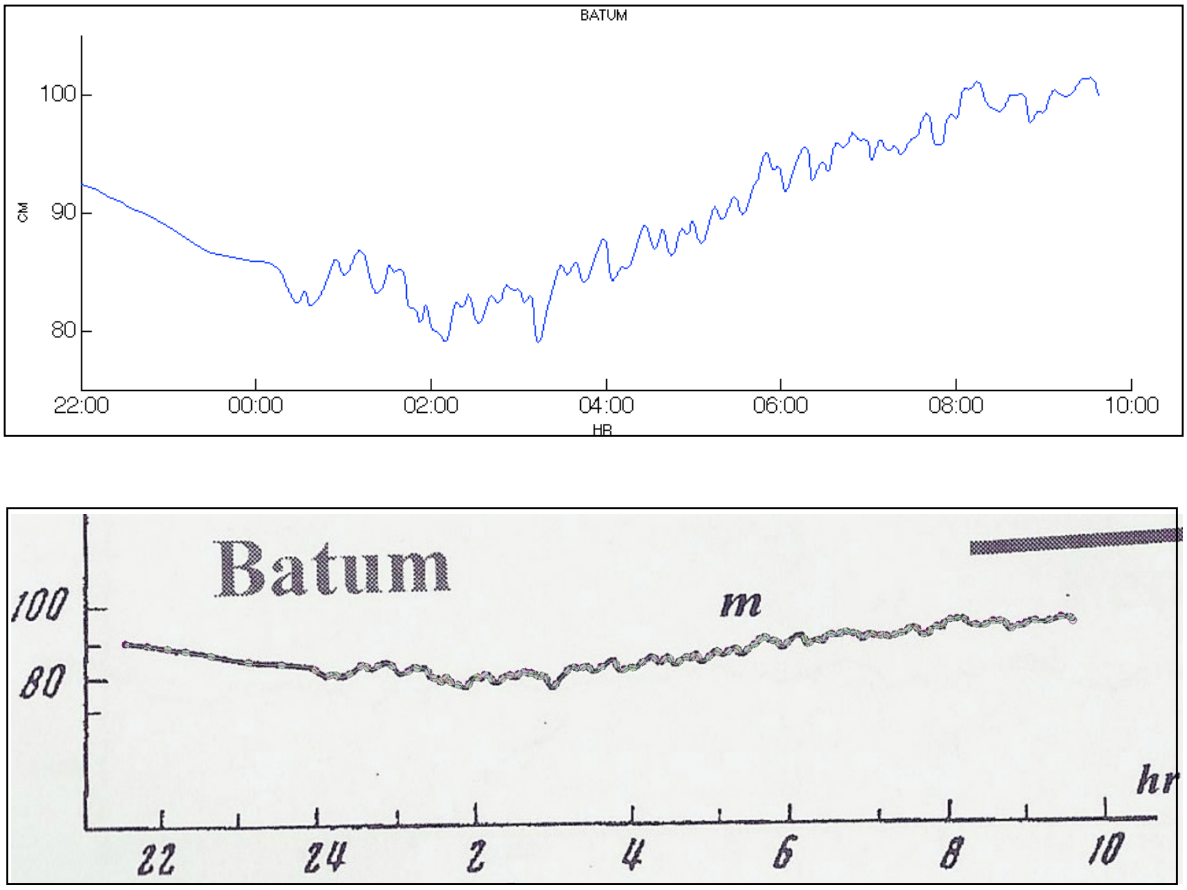

Figure 5.5.3. Batum digitized wave trace (above) and instrumental record (bottom).

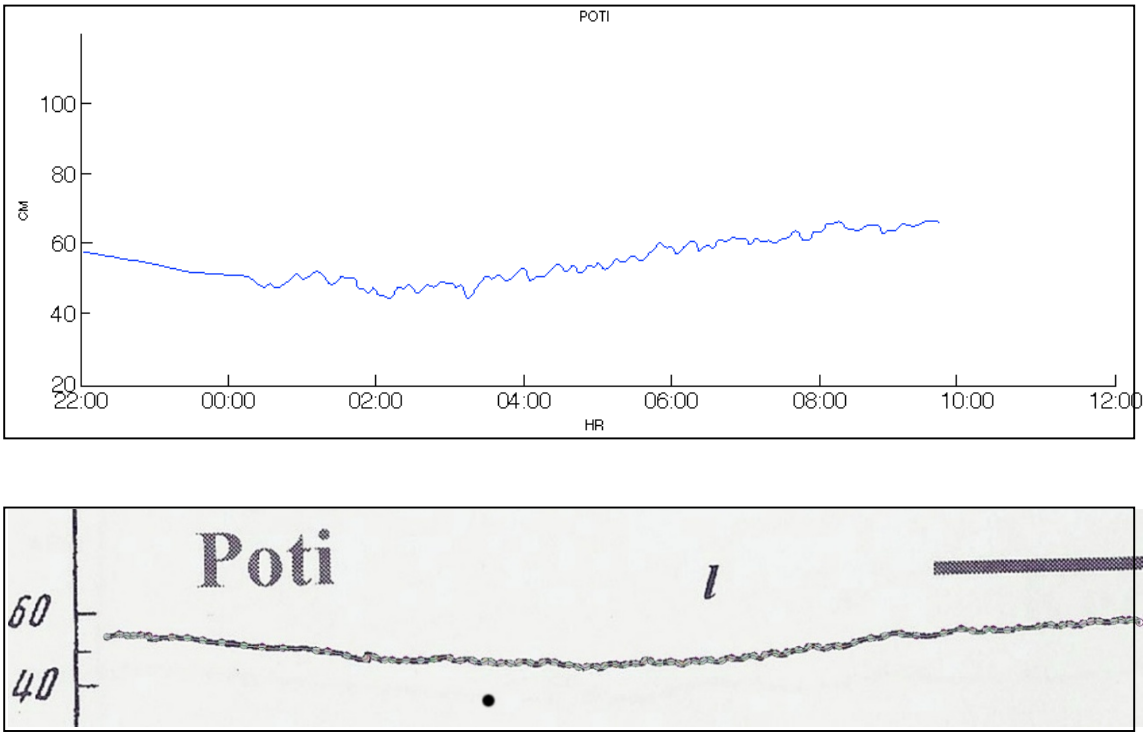

Figure 5.5.4. Poti digitized wave trace (above) and instrumental record (bottom).

6. CONCLUSIONS AND DISCUSSIONS

Bartın Earthquake provided the first seismological evidence for active thrust faulting in the southern margin of the Black Sea. Despite of intermediate size, the Bartın Earthquake caused some casualties and considerable damage in the towns of Bartın and Amasra and other villages in northwestern Turkey. The uplift of the water surface of the initial wave was calculated as 0.80 m. The amplitude of tsunami does not exceed 0.2 meters in almost all other gauge points. It was reported that the water surface elevation was maximum 40-50 cm which was based on the observations from inhabitants (Ketin *et al.,* 1969).

The 1939 Erzincan Earthquake is a very important earthquake that was recorded instrumentally. The significance of the NAFZ was first noticed with the occurrence of the 1939 Erzincan Earthquake (Pamir and Ketin, 1941 and Parejas *et al.,* 1942). The tsunami waves generated at Fatsa triggered by the Erzincan Earthquake. They approached the north coast between 40 min and 2.5 hours later. At the south coasts, maximum wave height is 0.58 m between Ordu and Fatsa towns. In addition, at the northwest and east coasts of the Black sea, wave heights were observed with lower values (app. 0.06 m). Tide gauge records from the Fatsa Tsunami recorded in the northern part of the Black Sea after the 1939 Erzincan Earthquake were compared with the results obtained from the tsunami numerical models and sufficient agreement was found in the arrival times of the wave in the North Black Sea. According to the compatibility of arrival time between the real data and numerical modeling result, it can be said that the location of landslide (source) is most probably correct and the model finds reliable results. In terms of the instrumental records, the arrival time of initial wave is 50.85 minutes and wave amplitude is 35 cm at Novorossiysk.

In this study, the comparison of modeling results can be compared with more tide gauge records. Finer bathymetry and topography can be used in the analyses. The alternative of the secondary can be modeled in addition to landslide case. In order to better satisfy correlation in the tsunami wave period in Novorossysk tide gauge record it is suggested that size of source dimension could be enlarged.

7. REFERENCES

Acır, O., V. I. Agoshkov, R. Aps, A. A. Danilov, and V. B. Zalesny, Y. Huang, 2013, "Potential Tsunami Hazard Modelling of Black Sea Coastline", *Turkey New Frontiers in Engineering Geology and the Environment*, DOI: 10.1007/978-3-642-31671-5_39, _ Springer-Verlag Berlin Heidelberg.

Albers, J. P. and A. Kalafatçıoğlu, 1969, "Bartın- Amasra Earthquake, Turkey, Sept. 3, 1968", *United States Geological Survey Project report* (IR) TU-5.

Alptekin, O., J. Nabelek and N. Toksöz, 1986, "Source Mechanism of the Bartın Earthquake of 3 September 1968 and Thoughts on Active Tectonics of the Black Sea", *Atmospheric and Planetary Sciences,* Massachusetts Institute of Technology, Cambridge, MA 02139 U.S.A.

Altınok, Y., 1999, *Tsunamis Along the Coasts of the Black Sea, 2"d Balkan Geophysical Congress and Exhibition*, in the Book of Abstracts, July 5-9, Istanbul, 46-47.

Altınok, Y., and S. Ersoy, 2000, "Tsunamis Observed on and Near Turkish Coast", *Natural Hazards*, Vo1.21, No 2-3, 185-205.

Ambraseys, N., and C. F. Finkel, 1995, *The Seismicity of Turkey and Adjacent Areas, A Historical Review*, 1500–1800, EREN Ltd, Istanbul, 240 pp.

Baptista, M. A., J. M. Miranda and J. F. Luis, 2006, "Tsunami Propagation a Long Tagus Estuary (Lisbon, Portugal) Preliminary Results", *Science of Tsunami Hazards,* University of Algarve, CIMA, Portugal., Vol. 24, No. 5, page 329.

Başarır, N., 2011, *Reassessment of the Seismic Parameters from Historical Seismograms of 1912-Mürefte-Şarköy, 1935-Erdek-Marmara Island and 1963-*

Çınarcık Earthquakes, M.S. Thesis, Kandilli Observatory and Earthquake Research Institute.

Bernard, E., H. O. Mofjeld, V. Titov, C. E. Synolakis and F. I. Gonzales, 2007, "Tsunami: Scientific Frontiers, Mitigation, Forecasting and Policy Implications", *Phil. Trans. R. Soc. A.,* 364.

Choi, B. H., B. I. Min, E. Pelinovsky, Y. Tsuji, and K. O. Kim, 2012, "Comparable Analysis of the Distribution Functions of Runup Heights of the 1896, 1933 and 2011 Japanese Tsunamis in the Sanriku area Choi", *Nat. Hazards Earth Syst. Sci.,* 12, 1463–1467.

Constantinescu, L. and V. Marza, 1989, "Long-term Strong Seismicity of Vrancea (Romania) Region", *Proceedings of the 21st ESC General Assembly*, 23–27 August 1988, Sofia, Bulgaria, 58–66.

Dobrychenko, A. V., M. P. Zaraiskii, N. V. Vandysheva, and N. V. Shebalin, 1975, *The Sochi Earthquake Swarm of 1969–1971, in the Soviet Union Earthquakes in 1971*, Nauka, Moscow, 36–45.

Dotsenko, S. F., 1995, "The Black Sea Tsunamis", *Izvestiya Atmospheric and Oceanic Physic,* 30(4), 483–489.

Dotsenko, S. F. and A. V. Konovalov, 1996, "Tsunami Waves in the Black Sea in 1927: Observations and Numerical Modeling", *J. Phys. Oceanography*, 7, 389–401.

Dotsenko, S. F. and A. V. Ingerov, 2007, "Characteristics of Tsunami Waves in the Black Sea According to the Data of Measurements", *Phys. Oceanography, 17, No. 1, 17–28.*

Dotsenko, S. F. and A. V. Ingerov, 2007, "Spectra of the Black-Sea Tsunamis", *Physical Oceanography*, Vol. 17, No. 5.

Dotsenko, S. F., and A. V. Ingerov, 2010, "Numerical Modeling Of The Propagation and Strengthenin of Tsunami Waves Near The Crimean Peninsula And The Northeast Coast Of The Black Sea", *Physical Oceanography*, Vol. 20, No. 1.

Ergünay, O., and A. Tabban, 1983, *Isoseismal Map of the Bartın Earthquake Based on the Official Damage Statistics of the General Directorate of Disaster Affair of the Government of Turkey*. Unpublished documents and map.

Grigorova, E. and B. Grigorov, 1964, "Earthquakes and Seismic Lines in Bulgaria", *Bulgarian Academy of Sciences*, Sofia, 83 pp., Bulgarian.

Grigorash, Z. K. and L. A. Korneva, "Tsunamis in the Black Sea", *International Tsunami Information Center, Newsletter*, Honolulu, Hawaii, 2, 2, 1969.

Grigorash, Z. K., 1972, "A Review of Distant Mareograms of Some Tsunamis in the Black Sea", *Trans. Sakhalrn Compex Sci. Rex Ins.,* 29, 271–278.

Kalafat, D., M Kara, K. Kekovalı, Y. Günes, P. D. Garip, S. Kuleli, L. Gülen, A. Pınar, N.M Özel, M. Yılmazer, 2005, "A Revised and Extended Earthquake Cataloque for Turkey Since 1900 (M>4.0)", *Bogaziçi Üniversitesi Yayınları* No=977, 558p. Bebek-Istanbul.

Ketin, I., 1948, "Die Grossen Anatolischen Erdbeben", *in den Letzten Zehn Jahren*. *Urania,* 11-Heft. 6-Jena.

Ketin I., and S. Abdüsselamoğlu, 1970, "Bartın Depremi'nin Etkileri", *Türkiye Jeoloji Kur. Bül*. 12, 66-76.

Kuşçu I., J. R. Parke, R. S. White, D. Mckenzie, G. A. Anderson, T. A. Minshull, N. Görür, ve A.M. Celal Şengör, 2004, "Active Slumping Offshore Amasra (Soutwest Black Sea) and Its Relation with Regional Tectonic", *Mineral Res Expl. Bull.* 128. 27-47.

Lander, J. F., 1969, "Seismological Notes – September and October 1968", *B. Seismol. Soc. Am*., 59, 1023–1030.

Mallet, R. and J. Mallet, 1855, *Catalogue of Recorded Earthquakes from 1606 BC to AD 1850*, *Brit. Assoc. Rep., London.*

Mckenzie, D., 1972, "Active Tectonics of the Mediterranean Region", *Geophysical Journal of Royal Astronomical Society*, 30, 109–185.

Murty, T.S., 1977, "Seismic Sea waves-Tsunamis", *Bulletin* 198, Fisheries Research Board of Canada, Ottawa, 337 Pages.

Nikonov, A., 1994, *Large Earthquakes and the Seismic Potential of the West Crimean (Sevastopol) Source Zone*, *Fiz. Zemli in Russian.*

Nikonov, A. A., 1997, "Tsunamis Occurrence on the Coasts of the Black Sea and the Sea of Azov, Izvestiya", *Physics of the Solid Earth*, 33, 77–87.

Nikonov, A. A., 1997, "Tsunami – a Threat from the South", *Science in Russia*, 6, 13–18.

Okada, Y., 1985, "Surface Deformation due to Shear and Tensile Faults in a Half-Space", *Bulletin of the Seismological Society of America*, 75:1135-1154.

Özel, M., Ö. Necmioğlu, A. Yalçıner, K. Doğan, E. and Mustafa, 2011, "Tsunami Hazard in the Eastern Mediterranean and Its Connected Seas: Towards a Tsunami Warning Center in Turkey", *Soil Dynamics and Earthquake Engineering*, 598–6.

Özer, C., 2012, *Tsunami Hydrodynamics in Coastal Zones*, Ph.D Thesis, Middle East Technical University.

Pamir, H. N., and I. Ketin, 1941, "Das Anatolische Erdbeben Ende 1939", *Geol. Rundschau,* Band 32, Heft 3- F. Enke-Stuttgart.

Panin, N., 1994, "Ecological Assessment of the Black Sea", *Razvedka I Ohrana Nedr, Moscova (in Russian)* T.33, 12, p.4-5.

Panin, N., 1996, "Danube Delta: Genesis, Evolution, Geological Setting and Sedimentology", *Geo-Eco-Marina*, 1, p.11-34, Bucuresti.

Papadopoulos, G. A., G. Diakogianni, A. Fokaefs, and B. Ranguelov, 2011, "Tsunami Hazard in the Black Sea and the Azov Sea: A New Tsunami Catalogue", *Nat. Hazards Earth Syst. Sci.*, 11, 945–963.

Papadopoulos, G. A. and F. Imamura, 2001, "*A Proposal for A New Tsunami Intensity Scale"*, *Proceedings International Tsunami Symposium*, Seattle, Session 5(5–1), 569–577.

Papadimitriou, E., V. G. Karakostas, 2008, "Rupture Model of the Great AD 365 Crete Earthquake in the Southwestern Part of the Hellenic Arc", *Acta Geophysica*, Volume 56, Issue 2, pp 293-312.

Parejas, I., M. Akyol, and E. Altınlı, 1942, "Le Tremblement de Terre d'Erzincan du 27 Decembre 1939 (secteur occidental)", *I.U¨.Jeoloji Enstitüsü*, 10, 187–222.

Pelinovsky, E., 1999, "Preliminary Estimates of Tsunami Danger for the Northern Part of the Black Sea", *Phys. Chem. Earth* (A), Vol. 24, No. 2, pp. 175-178.

Pintore, S., M. Quintiliani and D. Franceschi, 2005, "Teseo: A Vectorizer of Historical

Seismograms", *Computers & Geosciences, 31, 1277-1285.*

Ranguelov, B., 1996, "Seismicity and Tsunamis in the Black Sea", *Proc. of the 25th ESC General Assembly*, September 9–14, Reykjavik, Iceland, 667–673.

Ranguelov, B., 2003, *Possible Tsunami Deposits Discovered on the Bulgarian Black Sea Coast and Some Applications, in: Submarine Landslides and Tsunamis*, edited by: A. C. Yalçıner, E. Pelinovski, C. E. Synolakis, and E. Okal, Kluwer, 237–242.

Ranguelov, B., S. Tinti, G. Pagnoni, R. Tonini, F. Zaniboni, and A. Armigliato, 2008, "The Nonseismic Tsunami Observed in the Bulgaria Sea on 7 May 2007 – Was it due to a Submarine Landslide?", *Geophys*. Res. Lett., 35, L18613.

Richter, C. F., 1956, "Elementary Seismology", *Eurasia Publ. House (Pvt.) Ltd*., New Delhi.

Shuto, N., C. Goto, and F. Imamura, 1990, "Numerical Simulation as a Means of Warning for Near-Field Tsunamis", *Coastal Engineering in Japan*, 33(2), 173-193.

Von H., 1841, *Geschichte der Naturlichen Veranderungen der Erdoberflache, Chronik der Erdbeben und Vulcan-Ausbruche*, edited by: Gotha Perthes, J., 5, 406 pp., in German.

Wedding, H., 1968, "3 EyIül 1968'de Vukua Gelen Bartın-Amasra Yer Sarsıntısı", *MTA Dergisi*, 71, 135–141, 1968 in Turkish.

Yalçıner, A., E. Pelinovsky, T. Talipova, A. Kurkin, A. Kozelkov, and A. Zaitsev, 2004, "Tsunamis in the Black Sea: Comparison of the Historical, Instrumental, and Numerical Data", *J. Geophys. Res*., 109,C12023, doi:10.1029/2003JC002113.

Yalçıner AC, E. Pelinovsky, A. Zaytsev, A. Kurkin, C. Özer , H. Karakuş, 2006, *NAMI DANCE Manual*, METU, Civil Engineering Department, Ocean Engineering Research Center, Ankara, Turkey.